Cosmic-ray neutron soil moisture estimation using physically-based site-specific conversion functions

Mie Andreasen[1, 2], Karsten H. Jensen[2], Heye Bogena[3], Darin Desilets [4], Marek Zreda[5] and Majken C. Looms[2]

[1] Geological Survey of Denmark and Greenland, Copenhagen, Denmark

[2] Department of Geosciences and Natural Resource Management, University of Copenhagen, Denmark

[3] Agrosphere IBG-3, Forschungszentrum Juelich GmbH, Germany

[4] Hydroinnova LLC, Albuquerque, New Mexico, USA

[5] Department of Hydrology and Atmospheric Sciences, University of Arizona, USA

Corresponding author: Mie Andreasen (ma@geus.dk)

Key Points:

- CRN soil moisture can be estimated without calibration using oven-dried samples
- The proposed soil moisture conversion functions are dependent on the land cover type
- The land cover type can be determined from the thermal-to-epithermal neutron ratio

Abstract

In order to advance the use of the cosmic-ray neutrons (CRNs) to map soil moisture in heterogeneous landscapes, we need to develop a methodology that reliably estimates soil moisture without having to collect 100+ soil samples for each point along the survey route. In this study, such an approach is developed using physically-based modeling with the numerical MCNP neutron transport code. The objective is to determine site-specific conversion functions to estimate soil moisture from CRNs for the dominant land covers. Here, we assess this methodology at three field sites with similar mineral soil composition, but different land covers. First, we ensure that the developed models capture the most important differences in neutron transport behavior across sites. For this, we use measured time-series and height profiles of thermal and epithermal neutrons. Then, we compare the estimates obtained from the site-specific conversion functions with the standard N_0-calibration function. Finally, we compare the CRN soil moisture estimates with independent soil moisture estimates. Overall, the site-specific models are in agreement with the observed trends in neutron intensities. The site-specific soil moisture is similar to the N_0-estimated soil moisture, which results in comparable statistical measures. We show that various land covers have a significant impact on the amount and soil moisture sensitivity of epithermal neutrons, while the thermal neutrons are affected to a less degree. Thereby, thermal-to-epithermal neutron ratios can be used to identify the land cover type, and thereby the appropriate conversion function for soil moisture estimation for each point along the survey route.

1. Introduction

Soil moisture controls the exchange of energy and water at the ground-atmosphere interface. In particular, soil moisture influences the partitioning of solar energy into sensible and latent heat, and the separation of precipitation into runoff and infiltration. Therefore, robust observations of soil moisture are essential to study central hydrological processes like evapotranspiration and groundwater recharge.

High precision hectometer-scale soil moisture time series can be obtained using the cosmic-ray neutron (CRN) method based on the inverse relationship of background cosmic radiation (low energy neutrons) and hydrogen content (Andreasen et al., 2017a). The well-tested and robust N_0-calibration function is most often used for this conversion (Desilets et al., 2010). Only one unknown parameter needs to be determined, i.e. N_0, and the function combines information on geographic location, land cover type, soil chemistry, and sensor configuration. The N_0-parameter is estimated using 100+ soil samples collected within the CRN footprint at both dry and wet soil conditions (Franz et al., 2012). This procedure is most often possible for stationary soil moisture estimation. However, collecting proper samples in organic rich soils (e.g. litter), soils with many roots or rocks, and in clayey soils (especially at dry conditions) is difficult and sometimes impossible. Acquiring soil samples to estimate the N_0 parameter where both dry and wet soil conditions are represented is not always possible, especially if dry/wet conditions only occur rarely and at unpredictable times. Furthermore, the procedure of collecting 100+ soil samples often becomes cumbersome when mapping larger areas using the CRN rover.

CRN roving for soil moisture mapping has been demonstrated for regions of different land cover and soil characteristics, such as desert, grassland, and irrigated agricultural fields (Desilets et al., 2010; Chrisman and Zreda, 2013; Dong et al., 2014; Franz et al., 2015). Semi-empirical methods have been developed to account for effect of lattice water, soil organic matter and vegetation on neutron intensity. For example, Hawdon et al. (2014), Baatz et al. (2015) and Jacobi et al. (2018) presented extended versions of the standard N_0-calibration function to account for the moderation of CRNs by vegetation. Alternatively, Franz et al. (2013) developed the semi-theoretical universal calibration function where ancillary data on surface pressure, air temperature, relative humidity, soil bulk density, total biomass, lattice water and soil organic carbon is used to estimate CRN soil moisture (McJannet et al., 2014). Some of these data are not always readily available at the desired hectometer scale of observation.

Here, we present a novel approach to estimate soil moisture from CRN measurements that does not rely on calibration on oven-dried soil samples. The approach is an alternative to the standard N_0-calibration function for soil moisture estimation. The approach is expected to be relevant for soil moisture mapping using CRN roving in heterogeneous landscapes where an endless number of soil samples would be required to obtain reliable estimates using the standard N_0-calibration function. The methodology solely relies on numerical and physically-based neutron transport modeling of specific site conditions. We have previously documented the ability to model atmospheric profiles of thermal and epithermal neutron intensity at two sites representing two different land covers (Andreasen et al., 2016; 2017b). The models are based on information on the land cover (e.g. amount and height of the biomass and chemical composition of the vegetation) and the soil (e.g. soil layers, chemical composition, bulk density), and are most importantly not calibrated using soil sample

estimated soil moisture. In this study, the suite of models is extended to include the third most dominant land cover type in the area, heathland. First, the models are assessed by comparing measured and modeled neutron height intensities. By using two differently configured detectors, one without and one with moderator, a more exhaustive assessment of the models is obtained as thermal and epithermal neutrons have markedly different behavior and thereby information content. Secondly, models at dry and wet soil conditions are used to examine and quantify the sensitivity of thermal and epithermal neutron intensity profiles to soil moisture at each of the three field sites. Finally, ground level thermal and epithermal neutron intensities are modeled for different volumetric soil moisture values. These simulations are used to determine site-specific soil moisture conversion functions. To benchmark the approach, the soil moisture estimated using the site-specific conversion functions are compared to soil moisture estimated using the standard N_0-calibration functions. Furthermore, both CRN soil moisture datasets are compared to soil moisture measurements acquired from the soil sampling campaigns used to determine the N_0-parameters, and to soil moisture estimated by point-scale sensor networks setup within the CRN footprints and time-domain reflectometry (TDR) spatial measurement campaigns.

2. Field sites

Three field sites within the Danish hydrological observatory (HOBE) (Jensen and Refsgaard, 2018) are used for this study. The HOBE sites are situated on a glacial outwash plain within the Skjern River catchment in Jutland, western Denmark (see Figure 1). The soils are sandy, stratified, acidic, and poor in nutrients. Podzolation has formed a hardpan layer at 30 - 100 cm depth for large parts of the catchment. The sites are located within 10 km of each other at elevations of around 50 - 60 m above sea level and they are subject to similar climatic conditions. Also they have similar soil chemical composition but represent three contrasting land covers: farmland, heathland and forest, which typify the catchment.

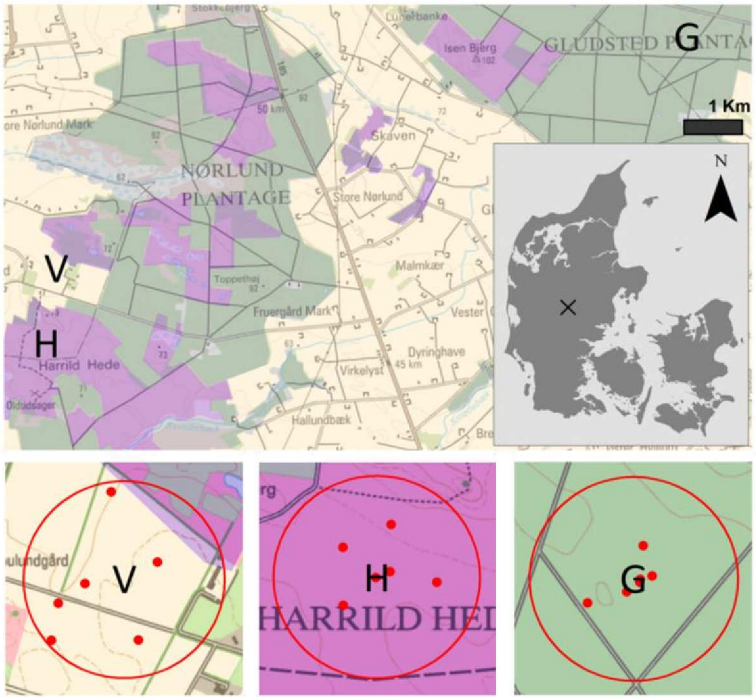

Figure 1. Field site locations for CRN intensity detection; H: Harrild Heathland (purple), V: Voulund Farmland (beige), and G: Gludsted Plantation (green). Point-scale soil moisture networks of six stations (red dots) are installed within the footprint of each neutron detector (red circle, radius = 300 m).

2.1. Voulund Farmland

Voulund (56°02'14"N 9°09'38"E) is an experimental farmland site, which has been deep-plowed to break the hardpan layer and improve drainage. For the past several years, the land has been cropped with spring barley, and is typically irrigated several times during spring and summer using approximately 20 mm/irrigation event. The wet above-ground biomass of spring barley was reported in 2013 to be 8 t/ha in the region (Statistics of Denmark, 2018). The approximately one-meter high crop is assumed to be composed of 85% water and 15% cellulose. The root zone is shallow (60 - 90 cm) (Refsgaard et al., 2011) and the wet below-ground biomass is estimated to 0.76 t/ha using the root-to-shoot ratio (the weight of the roots to the weight of the aerial part of the plant) for barley of 0.09 (Kwabiah et al., 2005). In the period between harvest in late summer and sowing in spring, crop residue is left on the fields (e.g., stalks and stubbles). Annual spring ploughing has homogenized the top 25-30 cm. This topsoil layer is dark and rich in organic matter in comparison to the underlying soil.

2.2. Harrild Heathland

Harrild Heathland field site (56°01'33"N 9°09'29"E) is a secondary HOBE field site established in the spring of 2014 for CRN measurements. This site is distinguished by low topography and the presence of a hardpan at 25-30 cm depth, which results in nearly saturated top-soils for most of the year. The site is covered by a mixture of grasses, small bushes and heather which have deposited a litter layer approximately 10-cm deep. The heathland is burned periodically to maintain the land cover type; however, the area around the field site has

not been burned since years before the field site was established. The wet above-ground biomass is assumed to be 9 t/ha (Härdtle et al., 2006) with 55% cellulose and 45% water.

2.3. Gludsted Plantation

The Gludsted Plantation (56°04'24"N 9°20'06"E) is a densely planted coniferous forest. The trees consist of rows of Norway spruce with small patches of Sitka spruce, Larch and Douglas fir. The plantation was established just before year 1900 and was deep-ploughed prior to forestation. The trees in the area of the field site are planted in the years 1962-1987 and has a maximum height of around 25 m. The dry above-ground biomass in the 38 ha vicinity of the CRN site was estimated to be 100 +/- 46 t/ha (one standard deviation) using LiDAR images from 2006 and 2007 (Nord-Larsen and Schumacher, 2012). In Scandinavian countries, Norway spruce typically has a stem-wood density of 0.83 g/cm^3 and generally 79% of the above-ground biomass is stored within the stem and 21% in the foliage. The root-to-shoot ratio for Norway spruce is 0.25 (Levy et al., 2004) providing an estimated dry below-ground biomass of 25 t/ha at the site. The dry matter of the tree form around 55% of the total weight and is primarily composed of cellulose, while the remaining 45% is water (Serup et al., 2002). The wet above-ground and below-ground biomass of the site area are estimated to be 182 t/ha and 45 t/ha, respectively. The root zone is assumed to reach down to 0.8 m (Refsgaard et al., 2011). The forest floor is characterized by a ~10 cm thick organic rich litter layer of needles, moss and other organic material.

3. Methods

3.1. Local soil characteristic

Soil sampling campaigns were conducted at the three field sites to obtain the necessary soil moisture data for N_0-estimation as well as chemical data for site-specific neutron transport modeling. Following the procedure proposed by Franz et al. (2013) soil samples were collected in 5 cm increments down to 30 cm at 18 locations surrounding the CRN detector. In total, 108 volumetric soil samples were obtained within an area of approximately 400 m by 400 m for each campaign. Soil moisture and dry bulk density for mineral soil samples were determined by oven-drying at 105°C for 24 hours. Organic rich soils were dried at 85°C for 48 hours to reduce charring of the organic material (O'Kelly, 2004). Based on the principles of the loss-on-ignition method (Ball, 1964), mineral soil samples were subsequently dried at 650°C and 900°C for the determination of the soil organic carbon content (SOC) and lattice water in the mineral grains and bound water, respectively. The concentration of major elements was measured with x-ray fluorescence spectrometry (XRF) (Weindorf et al., 2014).

Sampling campaigns were conducted at the three sites from May 2013 to October 2015. At Voulund Farmland, five campaigns were conducted; two during a fully grown spring barley crop, two after harvest (with stover) and one after ploughing (bare condition). At both Harrild Heathland and Gludsted Plantation, three campaigns were conducted. Area average water content and dry bulk density were calculated for the organic-rich litter layer and the mineral soil layers (Table 1). Mineral soil values are averages of 108 soil samples at Voulund Farmland. At Harrild Heathland and Gludsted Plantation, litter layer and mineral soil values are averages of 36 soil samples (18 locations and two depths) and of 72 soil samples (18 locations and four depths), respectively.

We have chosen to use the weighting scheme presented in Franz et al. (2013). It should therefore be noted that we do not necessarily account for nearby and shallow hydrogen sources, which could bias the result. However, the focus of this work is to compare different conversion functions. Applying a more advanced weighting scheme would affect both conversion functions similarly.

Table 1 is inserted here

The SOC content was measured at the three field sites (Table 1). At Voulund Farmland area average SOC was measured for the 0-30 cm depth interval using a composite sample of 108 soil samples. At Gludsted Plantation, SOC was measured on six randomly selected samples from two depth levels (10-15 cm and 25-30 cm). At Harrild Heathland, the area average SOC content was measured from a mixed sample of 72 soil samples in the top 20 cm mineral soil layer. The SOC content of the litter layer is assumed to be 100%. Small amounts of lattice water were measured (0.0009-0.0044 gram of water per gram of dry mineral soil) from the composite/mixed mineral soil samples also used for the determination of SOC at the three field sites. The XRF analysis for all three field sites were performed on two random soil samples collected at 20-25 cm depth. Details on the soil chemistry are provided in Table 2 and are included to highlight the similarity of the sites. The elemental composition of the soil is specified based on XRF analysis results, measured SOC content, estimated wet below-ground biomass and an assumed gadolinium concentration of 0.5 ppm. The gadolinium concentration is included because of its tendency to absorb thermal neutrons, as indicated by its high thermal neutron absorption cross-section (49000 barns; 1 barn = 10^{-24} cm^2), which is orders of magnitude higher than most soil elements. The presence of gadolinium can depress thermal neutron intensity even at low concentrations. The gadolinium concentration was measured from samples taken at a location of similar soil conditions close to the three field sites using inductively coupled plasma mass spectrometry (ICP-MC) (Salminen et al., 2005).

Table 2 is inserted here

3.2. Point-scale soil moisture sensing

Soil moisture time series were estimated using 5TE capacitance sensors (Decagon Devices Inc., 2014). The 5TE sensor elements are installed horizontally in the ground and measures apparent soil permittivity, temperature and bulk electrical conductivity simultaneously. The integrated measuring volume for apparent soil permittivity is approximately 20 cm^3 (Sakaki et al., 2008). According to the manufacturer, the 5TE sensor measures volumetric soil moisture and soil temperature with an accuracy of 0.03 and 1 ^{0}C, respectively. Data were logged every 30-min. Outliers were removed along with measurements conducted at soil temperatures below 1 ^{0}C to avoid measurements affected by frost. Topp´s equation (Topp et al., 1980) was used to estimate soil moisture from measured apparent soil permittivity in the mineral soil, while a site-specific petrophysical relationship (partly conducted at Gludsted Plantation and heathland areas nearby Harrild Heathland) was used for measurements conducted in the organic rich litter layers (Bircher et al., 2016).

In spring 2013 (Voulund Farmland and Gludsted Plantation) and spring 2014 (Harrild Heathland), six point-scale soil moisture stations were installed at each of the three field sites (Figure 1). At Voulund Farmland, two 5TE sensors were installed at 2.5 and 22.5 cm depths, respectively. Twice a year the stations were removed and

reinstalled to accommodate agricultural activities (harvest, ploughing and sowing) resulting in data-gaps and slightly changing conditions as the soil is prepared and the location of the station is changed slightly. For both Harrild Heathland and Gludsted Plantation, one 5TE sensor at each station was installed in the organic rich litter layer, whereas the other sensors were installed in the mineral soil at depths of 2.5 cm (one sensor) and 22.5 cm (two sensors).

In addition, a handheld TDR (Fieldscout TDR 300 Soil Moisture Meter, Spectrum Technologies, Inc.) was used to map soil moisture in the area of the CRN detectors. The TDR determines the dielectric constant used for soil moisture estimation based on the travel time of the electromagnetic pulses traveling along the TDR probes inserted in the soil. The measurements were made over the top 20 cm of the soil profile and each map consists of 121-163 measurement points collected within an area of 7-20 ha. According to the manufacturer, the expected accuracy of the soil moisture measurements is 0.03 m^3/m^3 at electrical conductivities below 2 mS/cm (Spectrum Technologies, Inc., 2017). Soil moisture was mapped 6-8 times at the three field sites in the period March to August 2016.

3.3. Cosmic-ray neutron intensity method

3.3.1. Neutron detectors

CRN intensity was recorded using a CRS1000/B system (Hydroinnova LLC, Albuquerque, NM, USA). The system consists of a moderated detector, an optional bare detector, and uses Hydroinnova's data logger with diagnostic capabilities for checking system health. Power is fed either from batteries (charged by solar panels) or directly by a power cable to the data logger. The data logger records barometric pressure, relative humidity and temperature inside and outside the detector enclosure for diagnostics and neutron intensity correction, respectively. The detectors have no direct contact with the ground, giving them a long operational life with low maintenance (Zreda et al., 2008; 2012). The detectors measure CRN primarily in the $<10^6$ eV energy range, where neutrons are strongly influenced by the absorption and elastic scattering properties of soil elements. The internal detector tubes utilize thermal neutron capture reactions, and hence the bare detector is preferentially sensitive to thermal neutrons with energies below 0.5 eV. The moderated detector includes a 2.5 cm HDPE moderator, which shifts the effective energy response toward epithermal neutrons with energies above 0.5 eV. The energy ranges measured by the detectors do not have sharp boundaries. As a consequence, the bare detector has an epithermal contribution of approximately 5% of the epithermal neutron intensity measured by the moderated detector, while the moderated detector has a thermal contribution of approximately 45% of the thermal neutron intensity measured by the bare detector (Andreasen et al., 2016). Poissonian statistics is the appropriate basis for the computation of the uncertainty of neutron intensity. The relative uncertainty decreases with increasing neutron intensity, N, and the standard deviation equals $N^{0.5}$ (Knoll, 2010).

3.3.2. Improving the detector characterization

To facilitate a comparison between model simulations and field measurements it is desirable to differentiate thermal and epithermal neutron intensity. A direct method to accomplish this is the cadmium difference method (Knoll, 2010; Andreasen et al., 2016). The cadmium difference method relies on two pairs of a bare and

a moderated detector. One detector pair is shielded by 0.5 mm thick cadmium foil (purity of 99.85%). The thermal neutron absorption cross-section (inversely related to the ability to transmit neutrons) of cadmium drops sharply from around 3500 barns to around 6.5 barns at an energy of 0.5 eV and remains low with increasing neutron energies. This leaves the cadmium shielded detectors sensitive only to epithermal neutrons (Knoll, 2010; Glasstone and Edlund, 1952). Thermal neutron intensity was calculated by subtracting the counting rate of the cadmium shielded bare detector from that of an equally sized bare detector. It was only practical to apply the cadmium-difference method for dedicated short-term field campaigns as the number of detectors required exceeded the number of detectors available at the individual sites. As an alternative to the cadmium difference method, correction models were used to estimate time-series of thermal and epithermal neutron intensities from the conventional bare and moderated detectors. The correction models used here were derived from field campaigns conducted at multiple locations and height levels (Andreasen et al., 2016). In order to estimate the epithermal neutron intensity during times where neutron intensity was only measured using the moderated detector, linear regression models were determined by relating the neutron intensity measured using the moderated neutron detector to the epithermal neutron intensity measured by the cadmium difference method. This was the case at all times at Harrild Heathland (2013-2019) and the period 2013-2016 at Voulund Farmland. Since the neutron intensity were detected using both bare and moderated detectors since 2016 at Voulund Farmland, the epithermal neutron intensity estimated using the regression function could be compared to the epithermal neutron intensity estimated using the correction models in the period 2016-2019. The time series of epithermal neutrons compare well (the results are not presented here).

Although the detectors utilized were nominally identical, small variations during manufacturing can lead to the tubes having slightly different efficiencies under identical conditions. Therefore, the first step of data processing was to normalize the raw CRN data (see also Andreasen et al., 2016).

3.3.3. Thermal and epithermal neutrons

We consider both thermal and epithermal neutrons, and expect different sensitivities to soil moisture for the two energy ranges at the three field sites. This is due to the different reaction patterns of thermal and epithermal neutrons and the different land cover characteristics in terms of the distribution of hydrogen and the elemental compositions of vegetation and soil. The production rate of epithermal neutrons per incident high-energy neutron increases with increasing atomic mass of the target element (Zreda et al., 2012), and most neutrons are therefore produced in the mineral soil where the heavier elements prevail. Absorption is the most significant reaction process for thermal neutrons, while scattering is a more important reaction for epithermal neutrons. For hydrogen, the thermal neutron absorption cross-section is around 0.32 barns, while the epithermal neutron scattering cross-section is around 20 barns (Zreda et al., 2012). Therefore, in the soil, the thermal neutron production rate is much higher than the absorption rate, while for epithermal neutrons both the production and scattering is substantial. In result, thermal neutron intensities have a maximum in the top 1 m of soil. Above the soil surface, the thermal neutron intensity first decrease sharply with height, reaches a minimum at the height at which the effect of the land surface becomes negligible, and then increases with increasing height. Except at very dry soil conditions the epithermal neutron intensity increases from the top soils and up through the atmosphere because soils have higher neutron scattering cross sections than air does (Zreda et al., 2012). Compared to the reaction pattern in the mineral soil, the production of epithermal

neutrons is low in the litter and vegetation material composed of lighter elements, while the moderation and absorption is high due to the high concentration of hydrogen. The increase in thermal (from some hundred meters height above the ground surface) and epithermal neutron intensity with height in the atmosphere reflects the cascade of high energy neutrons. The cascade is generated from primary cosmic-ray particles in the top of the atmosphere. Propagating the atmosphere, neutrons collide with and disintegrate nuclei. For every collision the neutron energy, and thereby the high energy neutron intensity, decreases (Zreda et al., 2012).

3.3.4. CRN experiments

We performed several experiments with the available CRN detectors at the three field sites to investigate the effects of land cover (i.e. vegetation, litter layer) on the neutron response to soil moisture changes. In order to improve our counting statistics, we used daily neutron intensity averages calculated on the hourly counting rates (Bogena et al., 2013). This was necessary because data at an hourly time-scale was rather noisy given the low neutron count rate of our low elevation field sites (50 - 60 m above sea level) and the available detector systems.

Low biomass case: Voulund Farmland

A moderated detector was installed at Voulund Farmland on February 7, 2013. Later, on January 12, 2016 a bare detector was added to the CRN setup of the field site. Thermal and epithermal neutron intensity were computed using our correction models at times with measurements of both bare and moderated detectors. In September and October 2015 CRN field campaigns were conducted using the moderated detector of Voulund Farmland together with the moderated and bare detectors normally installed at Gludsted Plantation. Using an 11-m high mast installed at the site, we obtained atmospheric profiles of neutron intensity at two height levels on September 22, 2015 (1.5 m and 10.75 m height) and three height levels on September 23, 2015 (1.5 m, 6 m and 10.75 m height) (Andreasen et al., 2016). Direct measurements of thermal and epithermal neutron intensity were obtained at the site from September 29 to October 20, 2015 using the cadmium-difference method. The fields were covered by stubble during the profile and cadmium difference measurements. One of the soil sampling campaign was conducted during the neutron intensity profile measurements on September 23, 2015, from which a mean volumetric soil moisture content of 0.22 was determined (Table 1).

Intermediate biomass case: Harrild Heathland

A moderated detector was installed at Harrild Heathland in March 20, 2014. Neutron intensity profiles could not be measured here due to the absence of a mast. From October 27 to November 16, 2015 thermal and epithermal neutron intensity were measured applying the cadmium-difference method using two bare detectors and one moderated detector. During this period, a soil sample campaign was conducted (on October 29, 2015) yielding an average volumetric water content of 0.38 (Table 1). The number of moderated detectors installed at Harrild Heathland has varied over time. From June 27, 2014 to September 22, 2015, and permanently from July 8, 2016 two moderated detectors were collecting data at the field site. During these times, the relative measurement uncertainty is lower due to the higher count rate.

High biomass case: Gludsted Plantation

Four neutron intensity detectors were installed on a 45-m high mast featuring Gludsted Plantation field site in February 8, 2013. A set of bare and moderated detectors were installed at ground level and canopy level (27.5-m height above the ground), respectively. Since the end of 2015, only the ground level set of bare and moderated detectors were installed at the field location. Atmospheric profiles of neutron intensity were measured at the site on November 25-26, 2013 and March 12-14, 2014 (details are provided in Andreasen et al., 2017b). Thermal and epithermal neutron intensity profiles were estimated from the respective bare and moderated counting rates using the correction models. Additionally, an epithermal neutron intensity profile was measured on March 12-14, 2014 using the cadmium shielded moderated detector. At the time of the profile the volumetric water content was 0.18.

3.3.5. Neutron correction and soil moisture estimation

CRN intensity from the CRS1000/B moderated detector was corrected for variations in barometric pressure, atmospheric water vapor and incoming neutron intensity (Desilets et al. 2010; Zreda et al., 2012; Rosolem et al., 2013). However, the bare detector was not corrected for atmospheric water vapor fluctuations. This seems to be justified by previous studies (Bethe et al., 1940; Lockwood and Yingst, 1956). Furthermore, preliminary modeling by the authors, and R. Rosolem (personal communication, 2015) suggest that ground level thermal neutron intensity is only weakly affected by atmospheric water vapor (up to 40% of the epithermal neutron correction but in the opposite direction and soil moisture dependent). More study of this effect is needed.

CRN intensity was converted to soil moisture using the standard N_0-calibration function (equation 1), derived from neutron transport modeling of epithermal neutrons (10-1000 eV) for pure silica soil and bare ground reference conditions (Desilets et al., 2010) and modified to include other sources of hydrogen than soil moisture (Zreda et al., 2012).

$$\theta(N) = \rho_b \left(\frac{a_0}{\frac{N}{N_0} - a_1} - a_2 - (\tau + SOC) \right) \quad (1)$$

where θ is the volumetric soil moisture, ρ_b is the dry bulk density of the soil in grams per cubic centimeter, N is the ground level epithermal neutron intensity in counts per time unit, N_0 is the ground level epithermal neutron intensity over dry soil in counts per time unit, τ is grams of lattice and bound water per gram of dry mineral soil, SOC is grams of water in organic matter per gram of dry mineral soil, and a_i are parameters; a_0 is 0.0808, a_1 is 0.372 and a_2 is 0.115. N_0 is recommended to be estimated from multiple soil moisture calibration campaigns representing both dry and wet conditions (Franz et al., 2012).

3.4. Modeling

3.4.1. Neutron transport model

To simulate the behavior of CRNs near the land surface we used the general purpose Monte Carlo N–Particle code version 6 (MCNP6) (Pelowitz, 2013). The code uses partially stochastic methods to simulate individual particle trajectories over a broad range of energies (10^{-11} - 20 MeV for neutrons). The code allows three-dimensional simulations for user-defined configurations and materials in cells of a structured geometric design.

MCNP6 utilizes nuclear cross-section libraries to compute probabilities of nuclear interactions and has been extensively benchmarked (Durkee and James, 2012).

We used MCNP6 to compute thermal (0-0.5 eV) and epithermal neutron fluxes (10-1000 eV) at volumetric soil moistures in the interval 0.05 – 0.50. The vertical extent of the model is ~2 km and the lateral domain is a square 400 x 400 m. The model is constrained by reflecting boundaries such that a particle hitting a model boundary will be reflected specularly back into the model domain. The neutron source is distributed along a plane coinciding with the top boundary surface, and has an energy spectrum that approximates the one reported by Hughes and Marsden (1966) but is limited to particles between 400 MeV and 50000 MeV. The detectors are cells extending across the horizontal extent of the domain. We simulated a minimum of three million particle histories per model run. These simulations yield the neutron flux per source particle, distributed by energy bin. In order to obtain values comparable to our measured counting rates we applied detector-specific empirical conversion factors for thermal and for epithermal neutrons (more details are provided in Andreasen et al., 2016).

To increase the vertical resolution of the cell flux tallies for the area of primary interest the thickness of the cells varies to give finer resolution near the land air-soil interface. From the ground surface to the upper boundary of the model domain the thickness of the cells increases from 0.5 m to 164 m. From the ground surface down to the lower boundary the thickness increases from 0.025 to 0.20 m.

Each cell is assigned a material of soil, vegetation or atmosphere. The lowest 4 m of the model consists of subsurface cells. Different soil materials are included to represent changing chemical compositions of subsurface layers with depth. The materials of the subsurface soil cells are determined from field measurements combined with literature values. From the ground surface and up, cells are assigned with an atmospheric material composed of 21% oxygen and 79% nitrogen by volume with a constant density of 0.001165 g/cm^3. Some runs also included vegetation. Here, the material and density of above ground cells are changed to represent vegetation instead of atmosphere. The vegetation is treated either as a homogenized layer or as a three-dimensional structure. For the later, sub-cells are included in the geometric structure to represent the spatial distribution of materials and densities of tree stem, foliage and the air in between the trees (Figure 2).

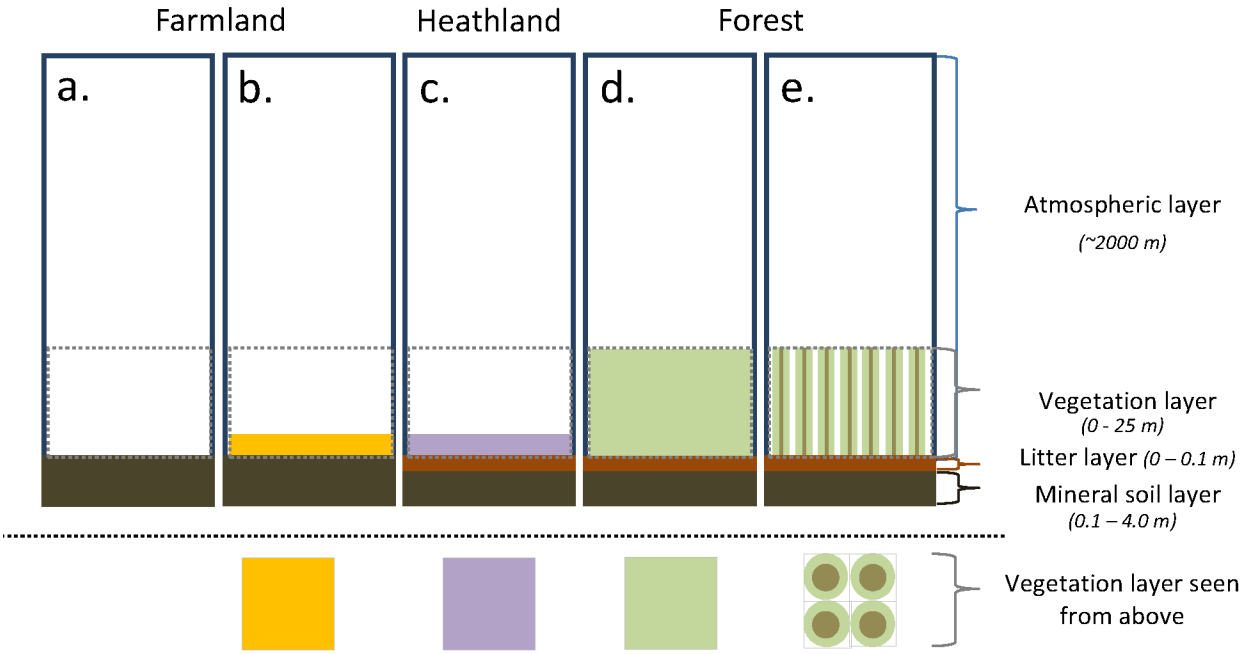

Figure 2. Vertical (above the dashed line) and horizontal (below the dashed line) model setup for Voulund Farmland (a. and b), Harrild Heathland (c.) and Gludsted Plantation (d. and e.) (adapted from Andreasen et al. (2017b)). The tree stems and foliage are not to scale for the illustration of the vegetation layer in representation e.

3.4.2. Site-specific neutron transport modeling

At each field site, two model setups are considered to investigate whether locale conditions affect the modeling results.

In the first Voulund Farmland model, we assume bare ground conditions, and the model is thus made entirely of air and soil (Figure 2A) (Andreasen et al., 2016). The soil is composed of a mixture of minerals, organic matter, water and air (Table 2). The second model is slightly more complex and represents a field with a fully-grown vegetation cover (Figure 2B). The crop layer is 1 m high and composed of the air in between the crops (density = 0.001165 g/cm^3), cellulose (density = 0.000126 g/cm^3) and water vapor (density = 0.000716 g/cm^3). The composite density is 0.002007 g/cm^3, as the biomass (8.42 t/ha) is assumed to be composed of 15% cellulose and 85% water. The soil chemistry in the top 0.3 m of the soil column includes the roots of the crop, while the soil chemistry from 0.3 to 4.0 m depth is the same as used for the bare ground model. The area average soil water content and dry bulk density (0-20 cm depth) determined from the soil sample field campaign conducted on 23 September 2015 is used for the modeling (Table 1). Soil chemistry data are provided in Table 2.

A 1 m thick vegetation is included for the Harrild Heathland model (Figure 2C). The vegetation material is composed of cellulose, water and air with a composite density of 0.002078 g/cm^3. The soil is a homogenized representation of the mineral soil material topped with a 10-cm-thick litter layer (cellulose and water). The

volumetric soil moisture and dry bulk density measured on 29 October 2015 was used. The area average volumetric water content was 0.38 (0-30 cm depth) and the dry bulk densities of the litter and the mineral soil were 0.876 g/cm^3 and 1.457 g/cm^3, respectively (Table 1). The dry bulk density of the litter layer is not expected to change over time. Nevertheless, significantly different values were measured probably due to measurement uncertainty related to the sampling and preparation of organic rich soil samples (O'Kelly, 2004). In order to test the influence of the measured range of litter layer dry bulk density on the thermal and the epithermal neutron intensity an additional model setup was applied. Apart from different dry bulk density of the litter layer the same model setup is used. The two models represents the lowest and highest measured dry bulk density of the litter layer (Table 1).

The Gludsted Plantation model includes soil, forest canopy and atmosphere. The soil is composed of five soil materials; one litter material (0.0-0.1 m depth), assumed to be 100% cellulose ($C_6H_{10}O_5$), and four mineral soil materials (0.1-4.0 m depth). The mineral soil materials consist of the major elements measured using XRF and different amounts of roots and SOC (see Tables 1 and 2). The material used for soil in 0.1-0.2 cm depth represents the root zone and contains a wet below-ground root biomass of 45 t/ha. The SOC content at this depth is 16.9%, while it in 0.2-0.3 m and 0.3-4.0 m depth is 7.6% and 0%, respectively. The area average dry bulk density as determined from the soil sampling field campaign on 26-27 August 2013 is used for the characterization of the litter and mineral soil layers (Table 1). Two model conceptualizations are used to describe the forest canopy layer with a dry above-ground biomass of 100 t/ha. The forest canopy layers extends from the ground to 25 m above the ground surface and is in the simple model-setup represented by a homogeneous layer made by an assembled material of cellulose and air with a composite density of 0.001892 g/cm^3 (Figure 2D). The more detailed model conceptualization includes three materials within the forest canopy layers: (1) tree stem with a density of 0.83 g/cm^3, (2) foliage including air with a composite density of 0.001510 g/cm^3, and (3) free air with a density of 0.001165 g/cm^3 (Figure 2E). The tree stem density and the distribution of biomass between tree stem and foliage represent typical values of Norway spruce (see section 2.3.). The trees have a stem diameter of 0.14 m, a surrounding cushion of foliage with a thickness of 1.70 m and a spacing of 2.36 m between the centers.

4. Results

4.1. Thermal and epithermal neutron height profiles

Measured and modeled thermal and epithermal neutron intensity height profiles at Voulund Farmland, Harrild Heathland and Gludsted Plantation are provided in Figure 3. The models include only information on soil chemistry, soil bulk density and vegetation, and are not calibrated.

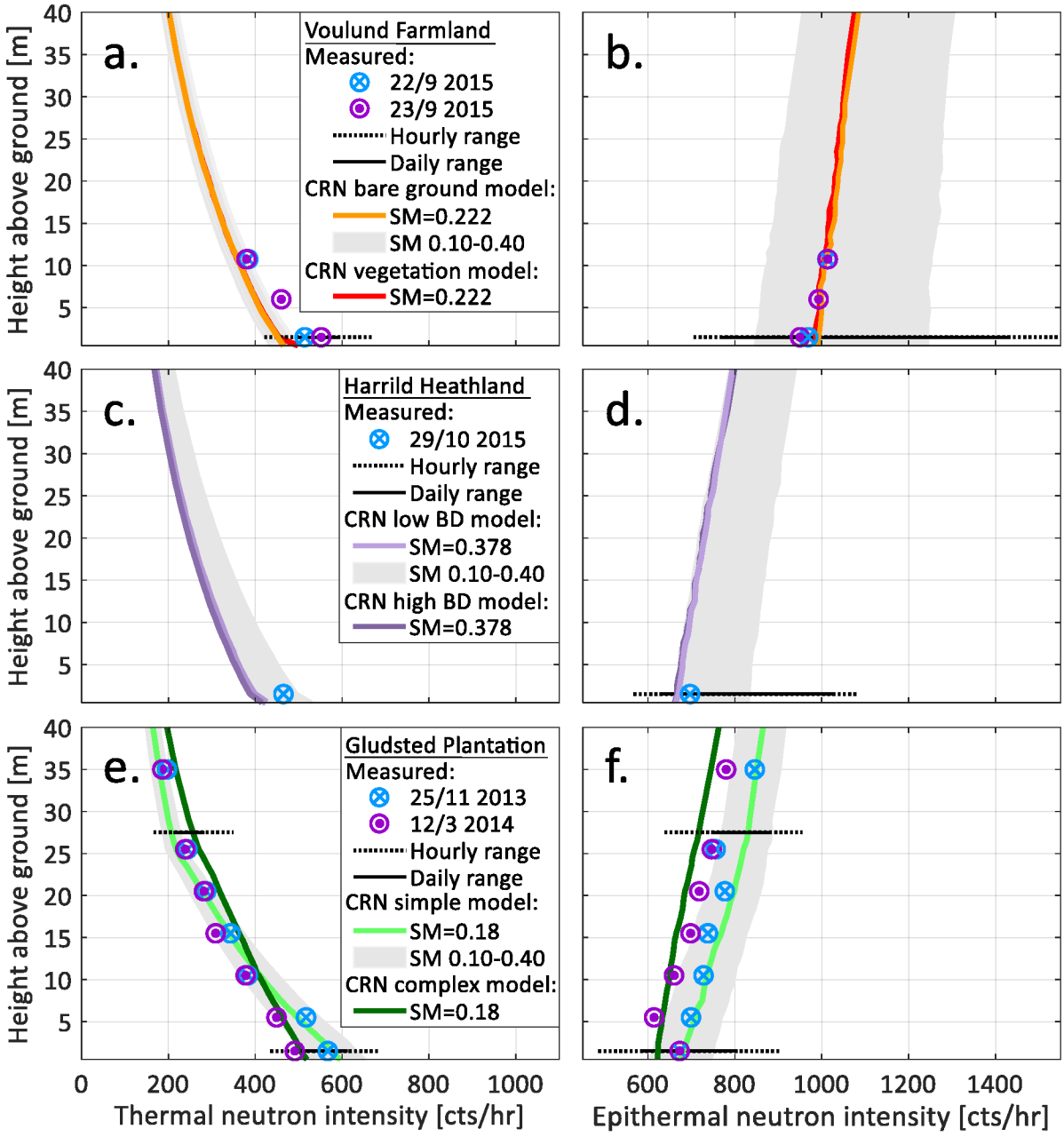

412

413 Figure 3. Measured and modeled thermal (left side) and epithermal neutron intensity profiles (right side) at
414 Voulund Farmland (a. and b.), Harrild Heathland (c. and d.) and Gludsted Plantation (e. and f.). The gray color
415 represents the range of modeled profiles for volumetric soil moistures (SM) 0.10 and 0.40 respectively for one
416 selected model setup at each field site. Hourly and daily ranges of neutron intensities are provided at one or
417 two height levels and for one or two neutron energy ranges.

418 Only small effects of changes in local conditions on neutron intensities are observed at Voulund Farmland
419 (Figures 3A and 3B) and at Harrild Heathland (Figure 3C and 3D). At Voulund Farmland, including a vegetation

cover resulted in a 0.4% increase in the ground level thermal neutron intensity and a 0.6% decrease in the ground level epithermal neutron intensity (compared to bare ground conditions). Thus, the seasonal variation in vegetation cover is not important at Voulund Farmland. For Harrild Heathland, the simulations appear rather insensitive to the dry bulk density of the litter layer for a volumetric soil moisture content of 0.38. For both field sites, a reasonable agreement between measured and modeled epithermal neutron intensity at ground level is obtained with a slight underestimation of thermal neutron intensity. The simulations for Voulund Farmland for heights are in good agreement with measurements. Larger differences appear for the thermal and epithermal neutron profiles modeled using a simple and a more detailed model setup at Gludsted Plantation. Overall, for the more complex model setup the slope of the neutron height profiles are steeper, and lower epithermal neutron intensities are modeled. Both of the modeled thermal neutron height profiles agree reasonably well with profile and time-series measurements at ground and canopy level for the time period 2013-2015 (Figures 3E). For the epithermal neutrons (Figures 3F), the height profile modeled using the simple model setup fits the profile measurements from November 2013 very well and also fall within the daily range of time-series measurements. The modeled epithermal neutron intensities are for most height levels either lower (the complex model setup) or higher (the simple model setup) than the neutron intensities measured in March 2014.

Thermal and epithermal neutron height profiles are very different at the ground-atmosphere interface and the three field sites show distinct differences, especially with respect to the epithermal neutron profiles. Overall, the sensitivity of thermal and epithermal neutrons to soil moisture vary among the three different field sites, and is quantified in absolute terms by calculating the difference in neutron intensity modeled at volumetric soil moisture values of 0.10 and 0.40. Considering the sensitivity using absolute values is important as the neutron count rate is important for the measurement uncertainty. Among the three field sites, the sensitivity to soil moisture at ground level for thermal neutrons is lowest at Voulund Farmland characterized by no litter layer and no vegetation (Figure 3A and Table 3). The sensitivity to soil moisture increases at Harrild Heathland (Figure 3C and Table 3) and Gludsted Plantation (Figure 3E and Table 3) due to the presences of a litter layer and increasing amounts of biomass. The differences between the field sites and the absolute sensitivity to soil moisture are reduced considerably with height (Figure 3A, 3C and 3E, and Table 3). Thermal neutrons are primarily generated in the ground and the thermal neutron intensity decreases with height as they are absorbed in the air, primarily by nitrogen. This causes a notable reduction in the absolute sensitivity with height. At some point (several hundred meters above the ground surface), the effect of the ground surface on thermal neutrons disappears resulting in an increasing thermal neutron intensity with height following the high energy cascade neutrons.

Table 3 is inserted here

As expected, the sensitivity to soil moisture is greater for epithermal neutrons than for thermal neutrons. At ground level, the range of epithermal neutrons at dry and wet soil is considerable smaller at field sites that include a litter layer and decreases even further as the amount of biomass becomes greater (Figures 3B, 3D and 3F, and Table 3). In the same manner, the hourly and daily ranges of ground level epithermal neutron intensity time-series measurement are greatest at Voulund Farmland, and are more than double of the time-

series measurement ranges at Gludsted Plantation (the field site with the lowest range of measurements). At ground level, the measurement ranges exceed the modeled ranges (represented by gray colored areas). This is expected as both lower volumetric soil moisture than 0.10 (e.g., during the long and dry summer in 2018) and higher volumetric soil moisture than 0.40 is likely at Harrild Heathland and Gludsted Plantation (high porosity in the top soil litter layers). At 40-m height above the ground surface the sensitivity to soil moisture on epithermal neutrons is modeled to be lower than at ground level, yet it is still significant (Figure 3 and Table 3). The model results demonstrate that the impact of surface characteristics is visible to much higher elevations for the epithermal neutrons than for the thermal neutrons (Figures 3B, 3D and 3F, and Table 3). The effect of soil wetness is apparent at considerably higher elevations for Voulund Farmland than for both Harrild Heathland and Gludsted Plantation. The height at which similar epithermal neutron intensities are achieved for Harrild Heathland and Gludsted Plantation is 500 m. All three field sites have approximately the same intensity at 700 m (results not presented here).

4.2. The relationship between low-energy neutrons and soil moisture

Figure 4 presents measured and modeled relationships between soil moisture and ground level neutron intensity of thermal and epithermal energies determined at Voulund Farmland (Figures 4A and 4B), Harrild Heathland (Figures 4C and 4D) and Gludsted Plantation (Figures 4E and 4F). Soil moisture measured from the soil sample field campaigns using oven drying, estimated by the sensor networks (soil column averages) and the handheld TDR are compared with both the thermal and epithermal neutron intensity. Relationships of soil moisture and epithermal neutron intensity using the standard N_0-calibration function (Desilets et al., 2010) are also provided by estimating the free parameter N_0 from the results of all soil sampling field campaigns conducted at the field sites.

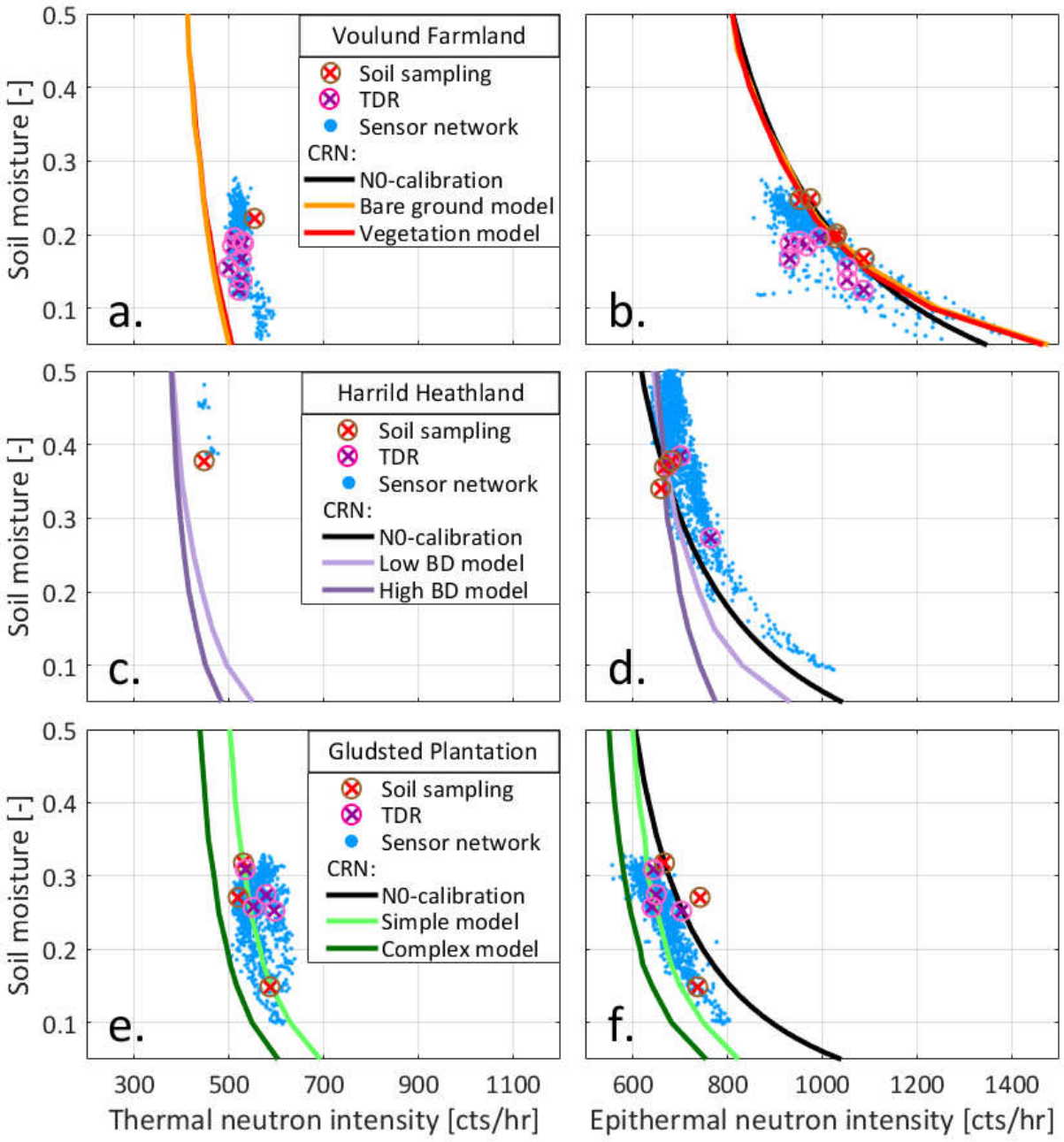

483

484 Figure 4. Site-specific modeling of the relationship between volumetric soil moisture, and ground level (1.5 m)
485 thermal (a., c. and e.) and epithermal neutron intensity (b., d. and f.), respectively, at Voulund Farmland,
486 Harrild Heathland and Gludsted Plantation. Modeling results are compared to CRN intensities and soil moisture
487 measured from volumetric soil sampling and oven drying, and estimated from soil moisture sensor networks
488 (soil column average) and from a handheld TDR. The data is provided as daily averages. Furthermore, the site-
489 specific modeling results (two models per field location, see Section 3.4.2. for details) are compared to the N_0-
490 calibration functions for soil moisture estimation using measurements of epithermal neutron intensity.

Overall, the site-specific models fit the independently acquired field data well (i.e. the soil sampling, the sensor network and the TDR), especially for the epithermal neutrons. The models are appropriate and well suited for the examination of the neutron transport at the three field sites as the modeling results match the observed trends (e.g. steepness of curves) and captures the overall shifts in the absolute thermal and epithermal neutron intensity between the sites. Distinct differences appear between the field sites with similar mineral soil chemistry and different land cover.

For Voulund Farmland similar relationships of soil moisture and neutron intensity (thermal and epithermal) are provided by the bare ground and vegetation models, suggesting that the seasonal change in land cover conditions (bare ground, stubbles or crop) is unimportant at all soil moisture conditions (Figures 4A and 4B). The modeled relationship of soil moisture and epithermal neutrons are also similar to relationship provided by the N_0-calibration function, despite at soil moisture below 0.15. A steeper curve is provided by the N_0-calibration function. Compared to the results obtained from field measurements the models slightly underestimate the relationship of soil moisture and thermal neutrons (Figure 4A). Overall, measured and modeled relationships of soil moisture and epithermal neutron intensity compare well (Figure 4B). The only exception is for the at all times slightly lower TDR soil moisture estimates.

At Harrild Heathland, different curves are obtained by the two models (Figures 4C and 4D). The models converge for wet soils for both thermal and epithermal neutrons but deviate substantially at the dry end. For this particular field site, the soil is predominantly wet throughout the year given a topographic low point and the presence of a hardpan layer in 25-30 cm depth. Furthermore the thermal neutron intensity was only measured during the wet conditions (0.38 – 0.48 m^3/m^3). At this soil moisture range, the two models underestimate the thermal neutron intensity by 50 - 60 cts/hr (Figure 4C). For both models, satisfactory agreement to epithermal neutron measurements is obtained for the wet regime, which is represented by all soil moisture measurements (soil sampling campaigns). More dry soil conditions are represented by the soil moisture estimates provided by the sensor network. The model results with the low bulk density litter layer are in good agreement with these measurements (Figure 4D). The relationship of soil moisture and epithermal neutrons provided by the standard N_0-calibration function and the site-specific model (low bulk density litter layer model) deviates increasingly as drier soil conditions are considered.

The model including a complex forest canopy conceptualization at Gludsted Plantation was expected to provide neutron intensity in better agreement with measurements as the local conditions are represented more accurately. Surprisingly, the best fit between measurements and modeling is obtained for the model based on a simple conceptualization of the forest layers (Figures 4E and 4F). This is especially true for thermal neutrons for which a remarkable agreement is obtained (Figure 4E). For the epithermal neutron intensity, the simple model compares well to measurements obtained by the sensor network and the TDR while it underestimates slightly when compared to soil sample measurements. The standard N_0-calibration function compares slightly better to the soil sampling soil moisture while it overestimates slightly when compared to the TDR soil moisture. Dry soil moisture conditions are mainly represented by measurements obtained by the sensor network. At soil moisture between 0.10 and 0.45 a range of epithermal neutrons of around 200 cts/hr is

measured. This is more in line with the range provided by the simple model (around 200 cts/hr) than the range provided by the standard N_0-calibration function (around 300 cts/hr).

4.3. Time series soil moisture estimation

Soil moisture are estimated from epithermal neutron measurements using the site-specific conversion function and the standard N_0-calibration function for each of the three field sites. For the determination of the site-specific conversion functions for CRN soil moisture estimation, curve fitting is conducted for the pairs of soil moisture and neutron intensity obtained by: (1) the bare ground model for Voulund Farmland, (2) the model with a relatively low dry bulk density of the litter layer for Harrild Heathland, and (3) the model including a simple forest conceptualization for Gludsted Plantation. For soil moisture estimation using the N_0-calibration function the dry bulk density of the top 20-cm was used. At Gludsted Plantation and Harrild Heathland these values tend to be low due to the predominance of light litter in the top layer consisting of plant material such as needles, bark and twigs. The N_0 parameter is estimated based on all the available soil sample field campaigns (Table 1). N_0 is determined to be 1475 cts/hr at Voulund Farmland, 1165 cts/hr at Harrild Heathland and 1244 cts/hr at Gludsted Plantation. Time-series of CRN soil moisture are compared with the soil moisture obtained from sensor networks (soil column average), the soil sampling and TDR field campaigns (Figure 5). Precipitation is measured at Voulund Farmland and Gludsted Plantation.

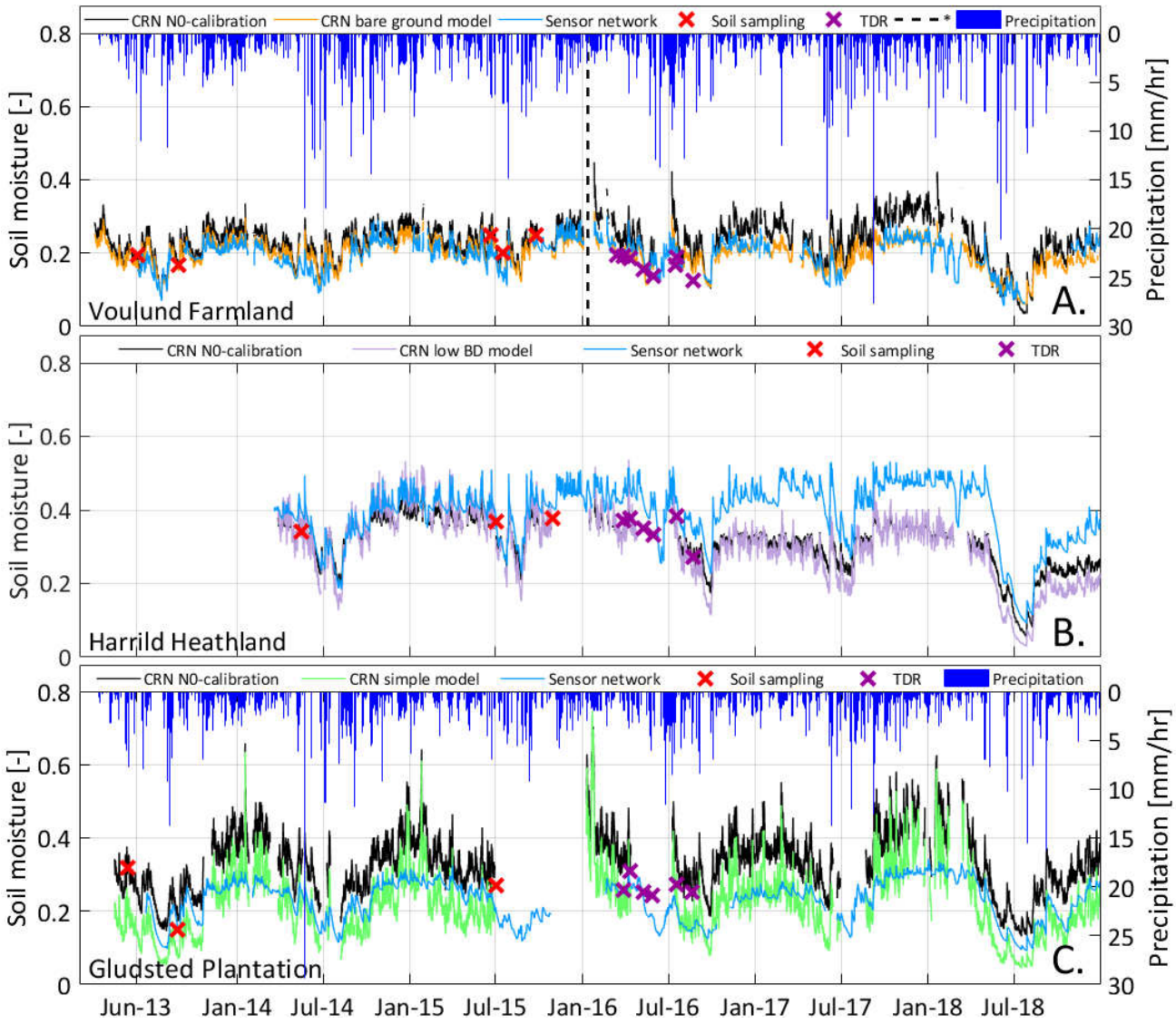

Figure 5. Time series of volumetric soil moisture obtained from CRN detection, sensor networks (soil column averages), soil sampling and TDR measurements for the period 2013 – 2019. The CRN soil moisture was estimated from ground level epithermal neutrons using the standard N_0-calibration function and the site-specific conversion function determined for the best performing CRN model for (A.) Voulund Farmland, (B.) Harrild Heathland, and (C.) Gludsted Plantation. Soil moisture estimates from the CRN detectors and sensor networks are daily moving averages. *The vertical dashed line at Voulund Farmland is included to show the day of transition (January 1 2016) between the two approaches used to obtain epithermal neutron intensity (regression model and correction model). More details are provided in section 3.3.2. CRN soil moisture at soil temperatures below and equal to 1 degree Celsius are taken out to remove spikes in the dataset. Hourly precipitation is included for Voulund Farmland and Gludsted Plantation.

Similar soil moisture estimates are obtained by the N_0-calibration function and the site-specific conversion function at Voulund Farmland (Figure 5A). However, slightly lower and less dynamic soil moisture values are provided by the site-specific conversion function compared to the N_0-calibration function from 2016. During this period the epithermal neutron intensity was estimated using the correction model and not using the regression function. The time-series are in satisfactory agreement with soil moisture from the sensor network, the soil sampling and the TDR campaigns. Larger differences in soil moisture estimates using ground level epithermal neutrons as well as the sensor networks are observed at Harrild Heathland and Gludsted Plantation (Figures 5 and 6). At Harrild Heathland, similar soil moisture are obtained from CRN measurements, soil sampling and TDR campaigns until the end of 2015. However from 2016, they start to deviate with higher sensor network soil moisture. Still, the dynamics are similar and the differences between the two methods are considerably smaller during summer. Soil moisture provided by the site-specific conversion function is more dynamic than soil moisture estimated using the standard N_0-calibration function. The responses of soil moisture estimated using the N_0-calibration function and the site-specific conversion function are similar at Gludsted Plantation. However, the estimates given by the site-specific conversion function are slightly more dynamic and are at all times (except one incidence in January 2016, probably due to a snow event) lower than the soil moisture provided by the standard N_0-calibration function. Overall, CRN soil moisture agree reasonable with soil moisture obtained from soil sampling and TDR campaigns. For the whole time period, the soil moisture estimated by the sensor network is at the same level as the soil moisture estimated by the site-specific conversion function. The dynamics are similar in summer, at times with a sharp drying curve (Figure 6). For the rest of year, the dynamic of the sensor network soil moisture is significantly lower than for the CRN soil moisture.

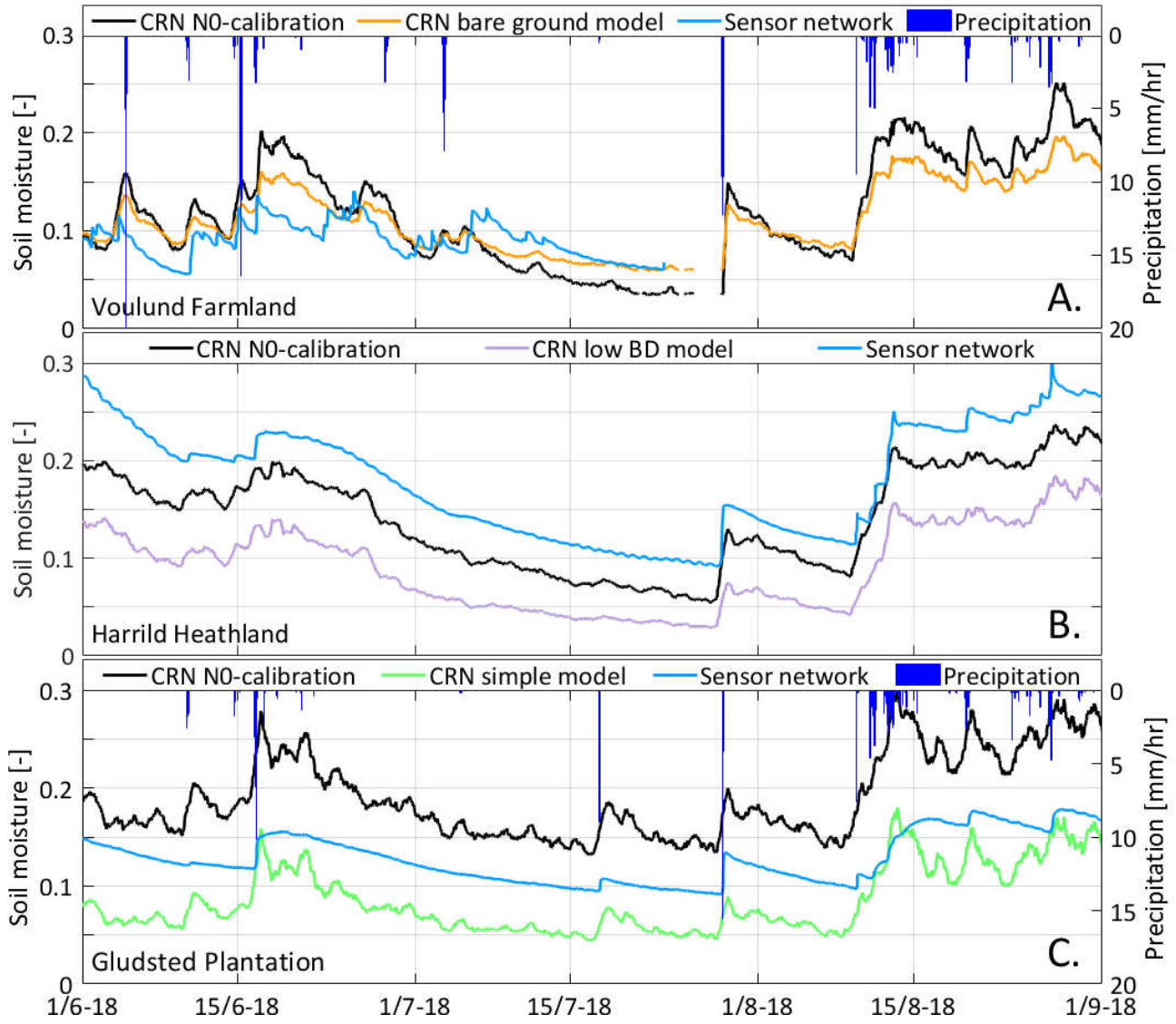

Figure 6. Time series of volumetric soil moisture obtained from CRN detection and sensor networks (soil column averages) for summer 2018. The CRN soil moisture was estimated from ground level epithermal neutrons using the standard N_0-calibration function and the site-specific conversion function determined for the best performing CRN model for (A.) Voulund Farmland, (B.) Harrild Heathland, and (C.) Gludsted Plantation. Soil moisture estimates from the CRN detectors and sensor networks are daily moving averages. Hourly precipitation is included for Voulund Farmland and Gludsted Plantation.

The soil moisture obtained from soil sampling (0-30 cm depth) and from the sensor network (in two or three depths, and the soil column average) are also used to quantify the performance of the site-specific conversion functions and the N_0-calibration functions for soil moisture estimation at the three field sites (Table 4). At Voulund Farmland, good linear model fit and statistics are archived comparing CRN soil moisture (both for the calibration and the conversion function), to soil sampling and sensor network soil moisture regardless of sensor

589 depth. This is obvious considering the slope values of the fitted linear model (being close to one), the high R^2
590 and the low rmse values.

591 **Table 4 is inserted here**

592 Overall, worse linear model fits and statistics are obtained comparing CRN soil moisture to soil moisture
593 obtained from soil sampling and sensor networks at Harrild Heathland and Gludsted Plantation than at
594 Voulund Farmland. This is expected as the field sites are more complex due to the land cover and larger
595 contrast in the composition of the soil layers as the soil is not prepared (e.g. ploughed). Also lower epithermal
596 neutron count rates result in higher relative uncertainty. At Harrild Heathland, negative slope values are
597 calculated for the linear models fitted to best describe the relationship of CRN and soil sampling soil moisture.
598 However, the expected positive slopes are obtained when the CRN soil moisture instead is compare to the
599 sensor network soil moisture (all depth levels). The statistics are similar for the N_0-calibration function and the
600 site-specific conversion function when related to each of the different sensor network depth levels and the soil
601 sampling measurements in 0-30 cm depth. It should be noted, that only the period 2014-2015 is considered
602 due to the sudden and unexplainable deviation in CRN and sensor network soil moisture from 2016 and
603 forward. At Gludsted Plantation, slope values close to one are achieved for the linear models fitted to the CRN
604 and soil sampling soil moisture datasets. However, low R^2 and relatively high rmse values are provided (Table
605 4). The statistics are better when comparing CRN soil moisture to sensor network soil moisture, especially for
606 the litter layer and the soil column average. All in all, the site-specific conversion functions and the standard N_0-
607 calibration functions perform equally well for soil moisture estimation at the three field sites.

608 # 5. Discussion

609 ## 5.1. Performance of site-specific conversion functions

610 The site-specific conversion function and the standard N_0-calibration function perform equally well for soil
611 moisture estimation at the three field sites. Overall, due to its simplicity and robustness, the standard N_0-
612 calibration function is preferable for soil moisture estimation. However, the approach proposed in this study
613 may prove valuable for situations where soil sampling for the determination of the N_0-parameter is impossible
614 or impractical. This applies to remote and inaccessible stationary field locations and CRN roving in
615 heterogeneous landscapes. In addition, neutron transport modeling can help us to gain insight and expand our
616 understanding of low-energy neutron transport. For example, somewhat surprising was the deviating soil
617 moisture estimates of the standard N_0-calibration function and the site-specific conversion function at Voulund
618 Farmland (Figure 4B). The added complexity of the soil chemistry was small, but nonetheless significant for the
619 relationship of soil moisture and epithermal neutron intensity at the dry end. It could be interesting to repeat
620 the study at a field sites with a much different soil properties to test if the effect of including the site-specific
621 soil chemistry would be more substantial for the resulting soil moisture estimates.

5.2. The land cover effect

Based on the neutron transport models of the three field sites, an examination of the effect of land cover on the sensitivity to soil moisture was enabled. This examination is important for CRN roving at heterogeneous landscapes. As expected, different sensitivities to soil moisture of thermal and epithermal neutrons were modeled (Figures 3-4, and Section 3.3.3.). The lower epithermal neutron intensity at Harrild Heathland and Gludsted Plantation (compared to Voulund Farmland) is both a result of the litter layers effective moderation of neutrons produced in the underlying mineral soil layers, as well as the overall higher concentrations of hydrogen within the detector footprint in the form of litter and vegetation. The litter and vegetation at Harrild Heathland and Gludsted Plantation is also the reason for the lower sensitivity to soil moisture on epithermal neutrons as the presence of more hydrogen pools dampens the signal of soil moisture. The moderation of epithermal neutrons in the litter layer causes the thermal neutron intensities to be higher at Harrild Heathland and Gludsted Plantation than at Voulund Farmland. Thereby, litter intensifies the response of thermal neutrons to soil moisture as higher count rates entail a higher absolute sensitivity to soil moisture.

5.3. Towards roving and airborne applications

In an earlier paper we reported an increasing thermal-to-epithermal neutron (t/e) ratio with added amounts of litter, SOC and biomass (Andreasen et al., 2017b). Information on the t/e ratio for different landscape units (Table 3) could be valuable for soil moisture mapping using CRN roving. For example, the detected t/e ratio could be used to identify the land cover type, and in turn, whether the conversion functions for Voulund Farmland, Harrild Heathland or Gludsted Plantation should be used. In addition, measuring the t/e ratio along the survey route, could potentially also be used for biomass mapping. These applications would require the CRN rover to include bare neutron detectors.

Very different height profiles for moderated and epithermal neutrons are measured because the thermal contribution to the moderated detector decreases substantially with height (Andreasen et al., 2016). Thus, the epithermal neutron intensity is increasing while the moderated neutron intensity is decreasing with height above the ground. For this reason, it is important to consider pure signals of thermal and epithermal neutrons if field experiments or CRN soil moisture mapping are conducted from a helicopter/UAV/tower where height levels may vary during a survey. For neutron detection from the air, the decreasing sensitivity of epithermal neutrons to soil moisture should also be considered. Reasonable soil moisture estimates were calculated from canopy level epithermal neutron intensity at Gludsted Plantation (results not presented here), despite of a reduction of approximately 20% in the sensitivity to soil moisture compared to ground level (Figure 3F and Table 3). For airborne neutron detection it may be necessary to consider higher elevations where the sensitivity of epithermal neutron intensity to soil moisture will be even lower. At 100 m height, the sensitivity of thermal and epithermal neutrons to soil moisture is reduced by 62% and 25% at Voulund Farmland, 89% and 36% at Harrild Heathland, and 82% and 29% at Gludsted Plantation, respectively.

5.4. Model performance

Up to the height of approximately 200 m, the thermal neutron intensity decreases with height above the ground surface (results not presented here). From that point on, and when the effect of the land surface soil on thermal neutrons is negligible, thermal and epithermal neutrons are in equilibrium and both increases with

height above the ground surface. The decreasing thermal neutron intensity and the increasing epithermal neutron intensity with height above the ground surface at the ground-atmosphere interface is successfully measured and modeled for all three field sites. This is remarkable considering the fact that no model calibration was made. The overall trends are well represented and the measured and modeled values compare well, especially for neutrons of epithermal energies.

The site-specific models for Harrild Heathland and Gludsted Plantation include multiple mineral soil layers with detailed information on soil chemistry, SOC and below ground biomass. Previous work suggest that this level of detail only affects the modeled thermal and epithermal neutron intensity to a small degree (Andreasen et al., 2017b). The largest effect on the neutron intensity was obtained when SOC was excluded. Here, the ground level neutron intensity increased with around 4%. Note, this is the case for a field site where the mineral soil is topped by a 10 cm thick litter layer. Perhaps specifications with a high degree of detail are important for field sites with no/thinner organic-rich top soil layer.

For all but one (i.e. the simple forest model), the site-specific models slightly underestimated the relationship of ground level thermal neutrons and soil moisture (Figure 4). The underestimation of thermal neutrons is similar for the three field sites (around 50-75 cts/hr) and could be a result of the conversion factor for thermal neutrons. The conversion factors, enabling modeled neutron intensities to be directly comparable to measured neutron intensities, were determined from measurements and modeling of CRNs at 0.5 m height above the water surface in Ringkøbing Fjord (a shallow brackish lagoon) located in the western part of Denmark (Andreasen et al., 2016). Only a single water sample was collected during the time of neutron intensity measurements to determine the water chemistry used in the Ringkøbing Fjord model. Andreasen et al. (2016) also modeled the neutron transport above seawater, and applying conversion factors based on this simulation increases the ground level thermal neutron intensity by 63-99 cts/hr at the three field sites for volumetric soil moisture 0.05-0.50 (results are not presented here). Therefore, the fit to measurements would be improved for all models (beside the simple forest model setup for Gludsted Plantation) if a conversion factor for more saline water were to be applied. In order to examine the applicability of the current thermal neutron conversion factor, we recommend that the field experiment conducted above a water body be repeated. To ensure a correct salinity estimate more water samples should be collected during the time of neutron measurements.

6. Conclusion

A novel methodology to convert CRNs to soil moisture was developed. Compared to the conventional N_0-method, the approach does not involve calibration using soil sampling. Instead site-specific neutron transport modeling using MCNP was used. For three selected sites, representing the most dominant land covers, the overall trends in thermal and epithermal neutron intensities were reproduced. The N_0-calibration and the site-specific conversion functions performed equally well, and were similar to independent estimates from soil sampling, point scale sensors and TDR measurements.

The developed method, using site-specific conversion functions, can be of great value at field sites where soil sampling is difficult or impossible due to a remote geographical location or due to problematic soil properties

(organic rich soils, soils with many roots or rocks, and impermeable dry clayey soils). However, most importantly, the approach could be a stepping stone for successful and reliable soil moisture mapping using CRN roving in heterogeneous landscapes where endless numbers of soil sampling is not feasible. As we gain knowledge on the impact of land cover on the neutron transport, relationships can be established that quantify the transition between the dominating land covers. A possible variable, that already has been shown to depend on land cover, is the thermal-to-epithermal neutron ratio.

7. Acknowledgements

We acknowledge The Villum Foundation (www.villumfonden.dk) for funding the HOBE project (www.hobe.dk). Lars M. Rasmussen and Anton G. Thomsen (Aarhus University) are greatly thanked for the extensive help in the field. Finally, we also acknowledge the NMDB database (www.nmdb.eu), founded under the European Union's FP7 programme (contract no. 213007) for providing data. Jungfraujoch neutron monitor data were kindly provided by the Cosmic Ray Group, Physikalisches Institut, University of Bern, Switzerland. Data used for this study are available from the PANGAEA data repository (Andreasen et al., 2019).

8. References

Andreasen, M., Looms, M. C, and Jensen, K. H. (2019), Cosmic-ray neutron intensity and soil moisture estimates in the period 2013-2019 at three field sites locations in the western part of Denmark. PANGAEA, doi: 10.1594/PANGAEA.909271.

Andreasen, M., Jensen, K.H., Desilets, D., Franz, T.E., Zreda, M., Bogena H.R., and Looms, M.C. (2017a), Status and perspectives on the cosmic-ray neutron method for soil moisture estimation and other environmental science applications. Vadose Zone J. 16(8), doi:10.2136/vzj2017.04.0086.

Andreasen, M., Jensen, K. H., Desilets, D., Zreda, M., Bogena, H., and Looms, M. C. (2017b), Cosmic-ray neutron transport at a forest field site: the sensitivity to various environmental conditions with focus on biomass and canopy interception, Hydrol. Earth Syst. Sci., 21, 1875–1894, doi: 10.5194/hess-21-1875-2017.

Andreasen, M., Jensen, K. H., Zreda, M., Desilets, D., Bogena, H. and Looms, M. C. (2016), Modeling cosmic ray neutron field measurements. Water Resour. Res., 52, doi: 10.1002/2015WR018236.

Baatz, R., H. R. Bogena, H.-J. Hendricks Franssen, J. A. Huisman, C. Montzka, and H. Vereecken (2015), An empirical vegetation correction for soil water content quantification using cosmic ray probes, Water Resour. Res., 51, doi:10.1002/2014WR016443.

Ball, D. F.: Loss-on-ignition as an estimate of organic matter and organic carbon in non-calcareous soils, J. Soil Sci., 15, 84–92, 1964.

Bethe, H. A., Korff, S. A. and Placzek, G. (1940), On the interpretation of neutron measurements in cosmic radiation. Phys. Rev., 57, 573–587.

Bircher, S., Andreasen, M., Vuollet, J., Vehviläinen, J., Rautiainen, K., Jonard, F., Weihermüller, L., Zakharova, E., Wigneron, J.-P. and Kerr, Y. H. (2016), Soil moisture sensor calibration for organic soil surface layers. Geosci. Instrum. Method. Data Syst, 5, 109–125, doi: 10.5194/gi-5-109-2016.

Bogena, H. R., Huisman, J. A., Baatz, R., Hendricks Franssen, H.-J. and Vereecken, H. (2013), Accuracy of the cosmic-ray soil water content probe in humid forest ecosystems: The worst case scenario. Water Resour. Res., 49, doi:10.1002/wrcr.20463.

Chrisman, B., and Zreda, M. (2013), Quantifying mesoscale soil moisture with the cosmic-ray rover. Hydrol. Earth Syst. Sci. 17:5097–5108. doi:10.5194/hess-17-5097-2013.

Decagon Devices Inc., ECH2O soil moisture sensor, Operator's manual for model 5TE, Decagon Devices Inc., 2365 NE Hopkins Court, Pullman, WA 99163, USA, 2014.

Desilets, D., Zreda, M. and Ferré, T. P. A. (2010), Nature´s neutron probe: Land surface hydrology at an elusive scale with cosmic rays. Water Resour. Res., 46, W11505, doi:10.1029/2009WR008726.

741 Dong, J., Ochsner, T.E., Zreda, M., Cosh, M.H. and Zou, C.B. (2014), Calibration and validation of the COSMOS
742 rover for surface soil moisture measurement. Vadose Zone J. 13(4). doi:10.2136/vzj2013.08.0148.

743 Durkee, J.W. and James, M.R. (2012), MCNP6 Verification and Validation for the MCNPX_65 and
744 MCNPX_EXTENDED Test Sets", LA-UR-12-00179.

745 Franz, T. E., Zreda, M., Rosolem, R. and Ferre, T.P.A. (2012), Field Validation of a Cosmic-Ray Neutron Sensor
746 Using a Distributed Sensor Network. Vadose Zone J., doi:10.2136/vzj2012.0046.

747 Franz, T. E., Zreda, M., Rosolem, R. and Ferre, T.P.A. (2013), A universal calibration function for determination
748 of soil moisture with cosmic-ray neutrons. Hydrol. Earth Syst. Sci., 17, 453–460, 2013, doi:10.5194/hess-17-
749 453-2013.

750 Franz, T.E., Wang , T., Avery, W., Finkenbiner, C. and Brocca L. (2015), Combined analysis of soil moisture
751 measurements from roving and fixed cosmic ray neutron probes for multiscale real-time monitoring. Geophys.
752 Res. Lett. 42:3389–3396. doi:10.1002/2015GL063963.

753 Glasstone, S. and Edlund, M. C. (1952), The elements of nuclear reactor theory. 5th Edn., Van Nostrand, New
754 York, 416 pp., 1952.

755 Hawdon, A., McJannet, D., and Wallace, J. (2014), Calibration and correction procedures for cosmic-ray neutron
756 soil soisture probes located across Australia, Water Resour. Res., 50, 5029–5043, 2014,
757 doi:10.1002/2013WR015138.

758 Hughes, E. B. and Marsden, P. L. (1966), Response of a standard IGY neutron monitor. Journal of Geophysical
759 Research, 71(5), 1435-1444, doi: 10.1029/JZ071i005p01435.

760 Härdtle, W., Niemeyer, M., Niemeyer, T., Assmann, T. and Fottner, S. (2006), Can management compensate for
761 atmospheric nutrient deposition in heathland ecosystems? Journal of Applied Ecology 2006 43, 759–769, doi:
762 10.1111/j.1365-2664.2006.01195.x.

763 Jacobi, J., Huisman, J. A., Vereecken, H., Diekkrüger, B. and Bogena, H. R. (2018), Cosmic ray neutron sensing
764 for simultaneous soil water content and biomass quantification in drought conditions, Water Resour. Res., 54,
765 7383-7402, doi: 10.1029/2018WR022692.

766 Jensen, K.H., Refsgaard, J.C. (2018), HOBE – the Danish Hydrological Observatory, Vadose Zone Journal,
767 17:180059, doi: 10.2136/vzj2018.03.0059.

768 Knoll, G. F. (2010), Radiation Detection and Measurement. Third Edition. John Wiley & Sons, Inc.

769 Kwabiah, A. B., Spaner, D. and Todd, A. G. (2005), Shoot-to-root ratios and root biomass of cool-season feed
770 crops in a boreal Podzolic soil in Newfoundland. Can. J. Soil Sci. 85: 369–376, doi: 10.4141/S02-032.

771 Levy, P.E., Hale, S.E. and Nicoll, B.C. (2004), Biomass expansion factors and root : shoot ratios for coniferous
772 tree species in Great Britain. Forestry, Vol. 77, No. 5, 2004, doi: 10.1093/forestry/77.5.421.

773 Lockwood, J. A., and Yingst, H. E. (1956), Correlation of meteorological parameters with cosmic-ray neutron
774 intensities. Phys. Rev., 104, 1718–1722.

775 McJannet, D., T. Franz, A. Hawdon, D. Boadle, B. Baker, A. Almeida, et al. (2014). Field testing of the universal
776 calibration function for determination of soil moisture with cosmic-ray neutrons. Water Resour. Res. 50:5235–
777 5248, doi:10.10022014WR015513.

778 Nord-Larsen, T. and Schumacher, J. (2012), Estimation of forest resources from a country wide laser scanning
779 survey and national forest inventory data. Remote Sensing of Environment 119 (2012) 148–157,
780 doi: 10.1016/j.rse.2011.12.022.

781 O'Kelly, B. (2004), Accurate determination of moisture content of organic soils using the oven
782 drying method, Drying Technology, 22(7), 1767-1776, doi: 10.1081/DRT-200025642.

783 Pelowitz, D. B. (2013), MCNP6^{TM} User´s Manual, Version 1. Los Alamos National Laboratory report LA-CP-13-
784 00634, Rev. 0.

785 Refsgaard, J.C., Stisen, S., Højberg, A.L., Olsen, M. etc. (2011), Vandbalance i Danmark- Vejledning i opgørelse af
786 vandbalance ud fra hydrologiske data for perioden 1990–2010. Danmark og Grønlands Geologiske
787 Undersøgelse Rapport 2011/77. Geol. Surv. of Denmark and Greenland, Copenhagen.

788 Rosolem, R., Shuttleworth, W. J., Zreda, M., Franz, T. E., Zeng, X. and Kurc, S. A. (2013), The Effect of
789 Atmospheric Water Vapor on Neutron Count in the Cosmic-Ray Soil Moisture Observing System. Journal of
790 hydrometeorology, doi: 10.1175/JHM-D-12-0120.1.

791 Sakaki, T., A. Limsuwat, K. M. Smits, and T. H. Illangasekare (2008), Empirical two-point a-mixing model for
792 calibrating the ECH2O EC-5 soil moisture sensor in sands, Water Resour. Res., 44, W00D08, doi:
793 10.1029/2008WR006870.

794 Salminen, R., Batista, M. J., Bidovec, M., Demetriades, A., De Vivo, B., De Vos, W. et al. (2005), Geochemical
795 Atlas of Europe. Part 1: Background Information, Methodology and Maps. Espoo, Geological Survey of Finland,
796 526 pages, 36 figures, 362 maps.

797 Serup, H., Falster, H., Gamborg, C., Gundersen, P., Hansen, L. Heding, N., Jakobsen, H. H., Kofman, P.,
798 Nikolaisen, L. and Thomsen, I. M. (2002), Wood for Energy production. Technology - Environment – Economy
799 Second Revised Edition.

800 Spectrum Technologies, Inc., Fieldscout TDR 300 soil moisture meter product manual Item # 6430FS, Spectrum
801 Technologies, Inc., 3600 Thayer Ct., Aurora, IL 60504, USA, 2017.

802 Statistics of Denmark (2018). Data is acquired from Statistics of Denmark, Tables HST77 and HALM1.

803 Topp, G.C., J.L. Davis, and A.P. Annan (1980), Electromagnetic determination of soil water content:
804 Measurements in coaxial transmission lines. Water Resour. Res. 16:574–582, doi: 10.1029/WR016i003p00574.

805 Weindorf, D.C., Bakr, N., and Zhu Y (2014), Advances in portable X-ray fluorescence (PXRF) for environmental,
806 pedological, and agronomic applications, Adv. Agron., 128, 1-45, doi:10.1016/B978-0-12-802139-2.00001-9.

807 Zreda, M., Desilets, D., Ferré, T. P. A. and Scott, R. L. (2008), Measuring soil moisture content non-invasively at
808 intermediate spatial scale using cosmic-ray neutrons. Geophysical Research Letters, Vol. 35, L21402, doi:
809 10.1029/2008GL035655.

810 Zreda, M., Shuttleworth, W. J., Zeng, X., Zweck, C., Desilets, D., Franz, T. and Rosolem, R. (2012), COSMOS: the
811 COsmic-ray Soil Moisture Observing System. Hydrol. Earth Syst. Sci., 16, 4079–4099, doi: 10.5194/hess-16-
812 4079-2012.

813

9. Tables

Table 1: Measured volumetric soil moisture, bulk density and SOC of the soil sample field campaigns conducted at Voulund Farmland, Gludsted Plantation and Harrild Heathland in the period 2013-2015. The average values of soil moisture and bulk density are provided along with standard deviations and ranges (minimum to maximum).

		Volumetric soil moisture [-]		Dry bulk density [g/cm^3]	
Site and sampling day, and SOC	Soil layer, depth in cm	Average (standard deviation)	Measurement range	Average (standard deviation)	Measurement range
Voulund Farmland					
3.6.2013 (bare ground)	Mineral, 0-30	0.188 (0.062)	0.066-0.313	1.419 (0.113)	1.150-1.631
29.8.2013 (stubbles)	Mineral, 0-30	0.141 (0.031)	0.055-0.201	1.293 (0.114)	1.035-1.553
19.6.2015 (crops)	Mineral, 0-30	0.222 (0.056)	0.080-0.394	1.447 (0.119)	1.132-1.716
16.7.2015 (crops)	Mineral, 0-30	0.161 (0.053)	0.062-0.278	1.375 (0.108)	0.951-1.576
23.9.2015 (stubbles)	Mineral, 0-30	0.222 (0.047)	0.140-0.315	1.472 (0.106)	1.152-1.760
SOC = 4.5%	Mineral, 0-30				
Harrild Heathland					
16.5.2014	Litter, 0-10	0.426 (0.187)	0.030-0.712	0.372 (0.296)	0.057-1.349
	Mineral, 10-20	0.296 (0.106)	0.107-0.655	1.146 (0.245)	0.399-1.535
1.7.2015	Litter, 0-10	0.527 (0.163)	0.194-0.827	0.788 (0.452)	0.180-1.532
	Mineral, 10-20	0.291 (0.130)	0.081-0.560	1.441 (0.168)	1.042-1.721
29.10.2015	Litter, 0-10	0.534 (0.161)	0.180-0.795	0.876 (0.435)	0.184-1.620
	Mineral, 10-20	0.300 (0.124)	0.057-0.542	1.457 (0.198)	0.862-1.762
SOC = 8.6%	Mineral, 10-30				
Gludsted Plantation					
14.5.2013	Litter, 0-10	0.420 (0.117)	0.183-0.689	0.663 (0.452)	0.131-1.525
	Mineral, 10-20	0.266 (0.087)	0.087-0.472	1.385 (0.198)	0.805-1.833
26-27.8.2013	Litter, 0-10	0.157 (0.072)	0.056-0.394	0.344 (0.291)	0.088-1.087
	Mineral, 10-20	0.145 (0.066)	0.055-0.392	1.090 (0.275)	0.221-1.530
3.7.2015	Litter, 0-10	0.360 (0.143)	0.115-0.758	0.649 (0.398)	0.168-1.485
	Mineral, 10-20	0.226 (0.099)	0.062-0.454	1.384 (0.221)	0.423-1.798
SOC = 16.9%	Mineral, 10-15				
SOC = 7.6%	Mineral, 25-30				

Table 2: The chemical composition of major elements at Voulund Farmland, Harrild Heathland and Gludsted Plantation determined using x-ray fluorescence (XRF) analysis on soil samples collected in approximately 25 depth. Bdl: Below detection limit of XRF analysis.

	Voulund Farmland [mass%]	Harrild Heathland [mass%]	Gludsted Plantation [mass%]
O	52.32	52.76	52.78
Si	42.65	44.71	44.86
Al	3.29	1.74	1.54
K	0.86	0.56	0.53
Ti	0.20	0.23	0.29
Ca	0.33	bdl	bdl
P	0.24	bdl	bdl
Fe	0.12	bdl	bdl

Table 3: Thermal and epithermal neutron intensity, and the t/e ratio at soil moisture (SM) 0.10 and 0.40 at 1.5-m and 40-m height above the ground surface for the bare ground model (Voulund Farmland), the low dry bulk density litter layer model (Harrild Heathland) and the simple forest conceptualization model (Gludsted Plantation).

		Thermal neutrons [cts/hr]			Epithermal neutrons [cts/hr]			t/e ratio	
	Height [m]	SM 0.10	SM 0.40	Difference	SM 0.10	SM 0.40	Difference	SM 0.10	SM 0.40
Voulund Farmland	1.5	483	423	60	1243	851	392	0.39	0.50
	40	221	187	35	1303	958	346	0.17	0.20
Harrild Heathland	1.5	496	394	102	831	664	167	0.60	0.59
	40	212	170	42	938	790	148	0.23	0.22
Gludsted Plantation	1.5	630	514	116	749	614	135	0.84	0.84
	40	179	150	29	914	810	105	0.20	0.19

Table 4: Linear model fit (slope and intercept) and statistics (R^2 and rmse) of soil moisture determined from soil sampling and sensor networks, and CRN measurements at Voulund Farmland (2013-2019), Harrild Heathland (2014-2015) and Gludsted Plantation (2013-2019). For the sensor network, measurements from the litter layer (not Voulund Farmland), 2.5 cm and 22.5 cm depth in the mineral soil, as well as an average for the whole soil column are used. For the CRN measurements, soil moisture are estimated using the standard N_0-calibration and the site-specific conversion functions for the three field sites. Neutron intensity measurements at soil temperatures below and equal to 1 degree Celsius (for the top 5 cm soil layer) are not included in the used dataset.

842

		Voulund Farmland		Harrild Heathland		Gludsted Plantation	
Soil sampling		N_0-calibration	Site-specific conversion	N_0-calibration	Site-specific conversion	N_0-calibration	Site-specific conversion
0-30 cm depth	Slope	0.80	0.95	-0.73	-0.43	0.95	1.02
	Intercept	0.043	0.032	0.624	0.521	0.013	0.114
	R^2	0.955	0.955	0.816	0.825	0.467	0.477
	rmse	0.010	0.023	0.036	0.050	0.052	0.127
Sensor network							
Litter layer	Slope	-	-	0.53	0.84	0.86	0.89
	Intercept	-	-	0.072	-0.082	0.061	-0.060
	R^2	-	-	0.802	0.787	0.721	0.669
	rmse	-	-	0.181	0.172	0.054	0.108
2.5 cm depth	Slope	1.13	0.80	0.62	0.99	1.43	1.49
	Intercept	0.025	0.052	0.142	0.025	0.064	-0.059
	R^2	0.795	0.756	0.847	0.845	0.568	0.539
	rmse	0.055	0.028	0.035	0.037	0.154	0.071
22.5 cm depth	Slope	1.13	0.83	1.13	1.79	1.37	1.41
	Intercept	-0.001	0.027	0.042	-0.128	0.052	-0.068
	R^2	0.697	0.714	0.789	0.771	0.583	0.538
	rmse	0.041	0.025	0.081	0.098	0.142	0.070
Average	Slope	1.19	0.86	0.71	1.13	1.26	1.30
	Intercept	0.001	0.032	0.080	-0.071	0.036	-0.086
	R^2	0.796	0.788	0.831	0.819	0.702	0.654
	rmse	0.046	0.021	0.041	0.041	0.107	0.056

843

844

845

846

847

848

Figure 1.

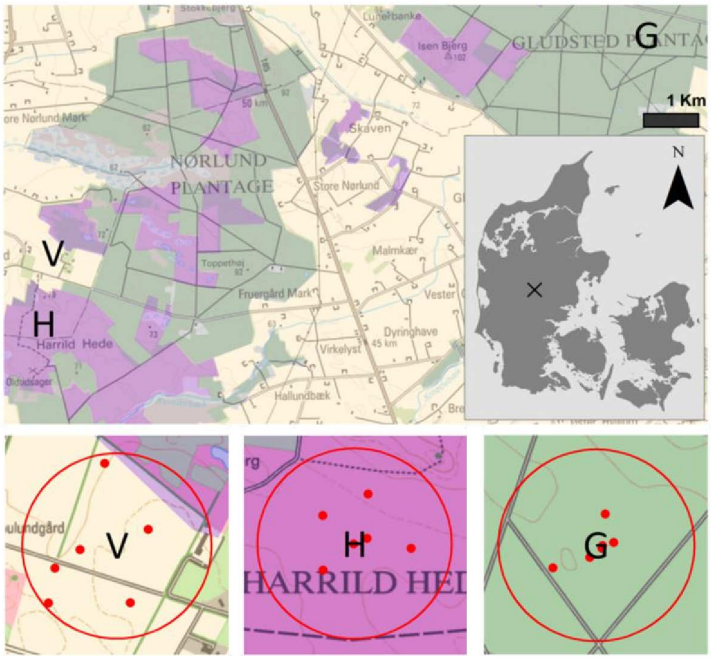
G
1 Km
N
NØRLUND
PLANTAGE
Store Nørlund
Skaven
Malmkær
Vester
Dyringhave
45 km
Virkelyst
Hallundbæk
Fruergård Mark
Toppethøj
Harrild Hede
V
H

Figure 2.

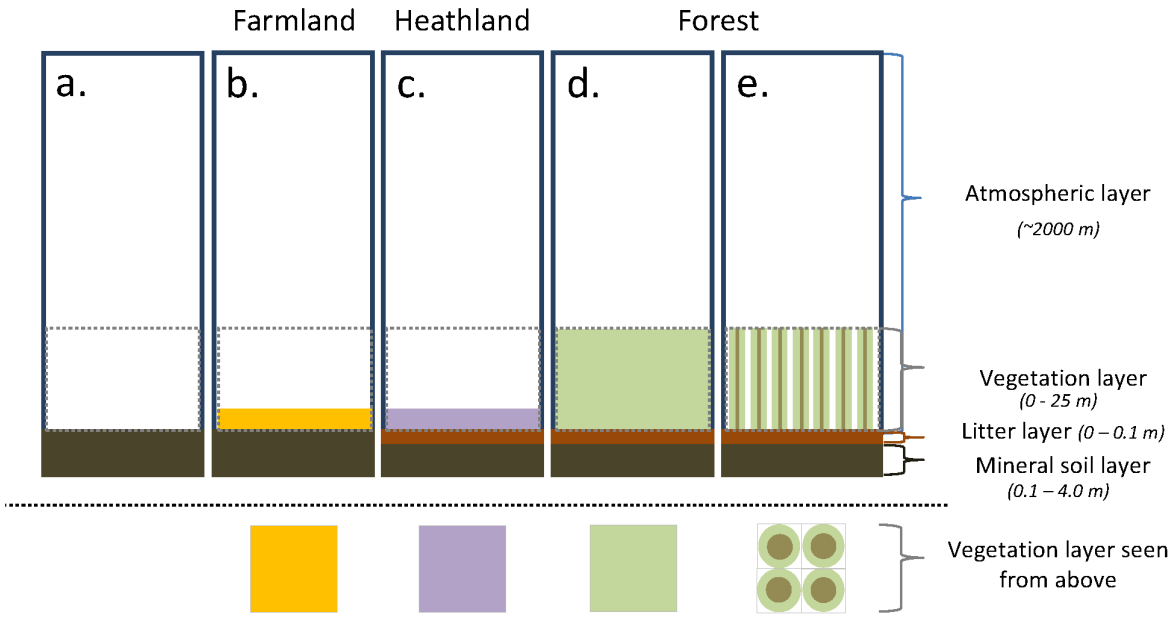
Farmland
Heathland
Forest
a.
b.
c.
d.
e.
Atmospheric layer
(~2000 m)
Vegetation layer
(0 - 25 m)
Litter layer (0 – 0.1 m)
Mineral soil layer
(0.1 – 4.0 m)
Vegetation layer seen from above

Figure 3.

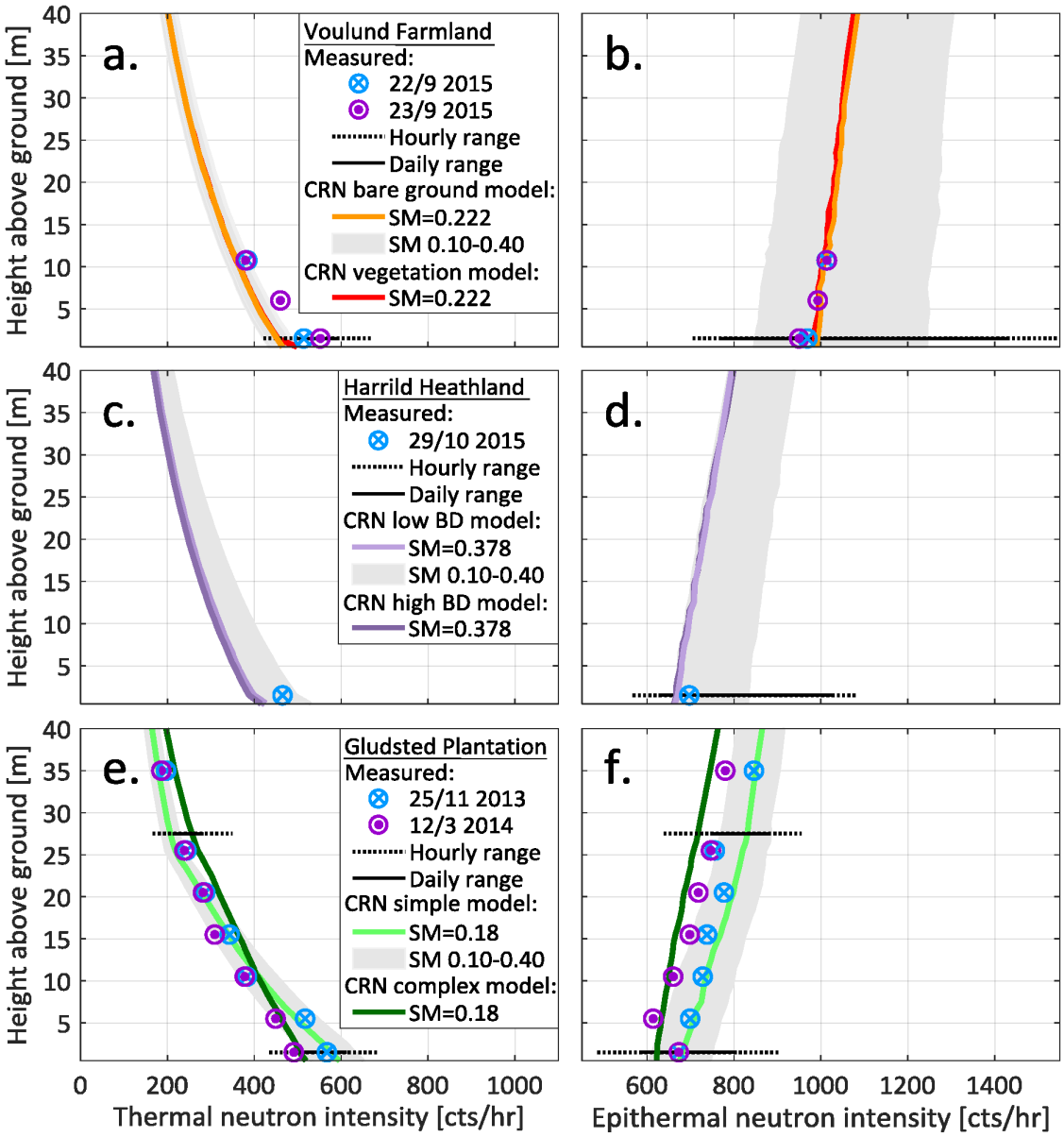
a.
b.
c.
d.
e.
f.
Voulund Farmland
Measured:
22/9 2015
23/9 2015
Hourly range
Daily range
CRN bare ground model:
SM=0.222
SM 0.10-0.40
CRN vegetation model:
SM=0.222
Harrild Heathland
Measured:
29/10 2015
Hourly range
Daily range
CRN low BD model:
SM=0.378
SM 0.10-0.40
CRN high BD model:
SM=0.378
Gludsted Plantation
Measured:
25/11 2013
12/3 2014
Hourly range
Daily range
CRN simple model:
SM=0.18
SM 0.10-0.40
CRN complex model:
SM=0.18
Height above ground [m]
Thermal neutron intensity [cts/hr]
Epithermal neutron intensity [cts/hr]

Figure 4.

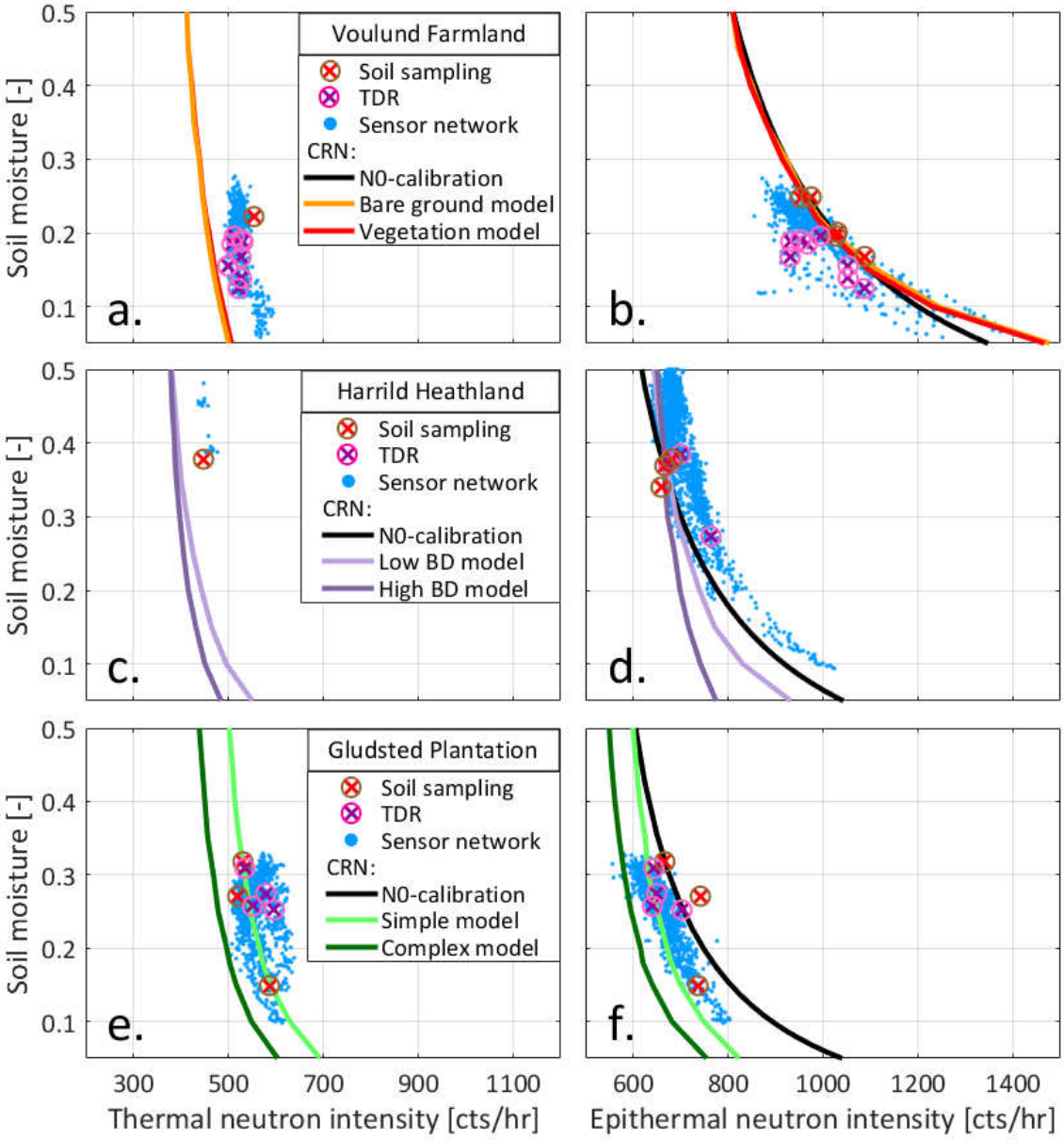
Voulund Farmland
Soil sampling
TDR
Sensor network
CRN:
N0-calibration
Bare ground model
Vegetation model
a.
b.
Harrild Heathland
Soil sampling
TDR
Sensor network
CRN:
N0-calibration
Low BD model
High BD model
c.
d.
Gludsted Plantation
Soil sampling
TDR
Sensor network
CRN:
N0-calibration
Simple model
Complex model
e.
f.
Soil moisture [-]
0.5
0.4
0.3
0.2
0.1
300
500
700
900
1100
Thermal neutron intensity [cts/hr]
600
800
1000
1200
1400
Epithermal neutron intensity [cts/hr]

Figure 5.

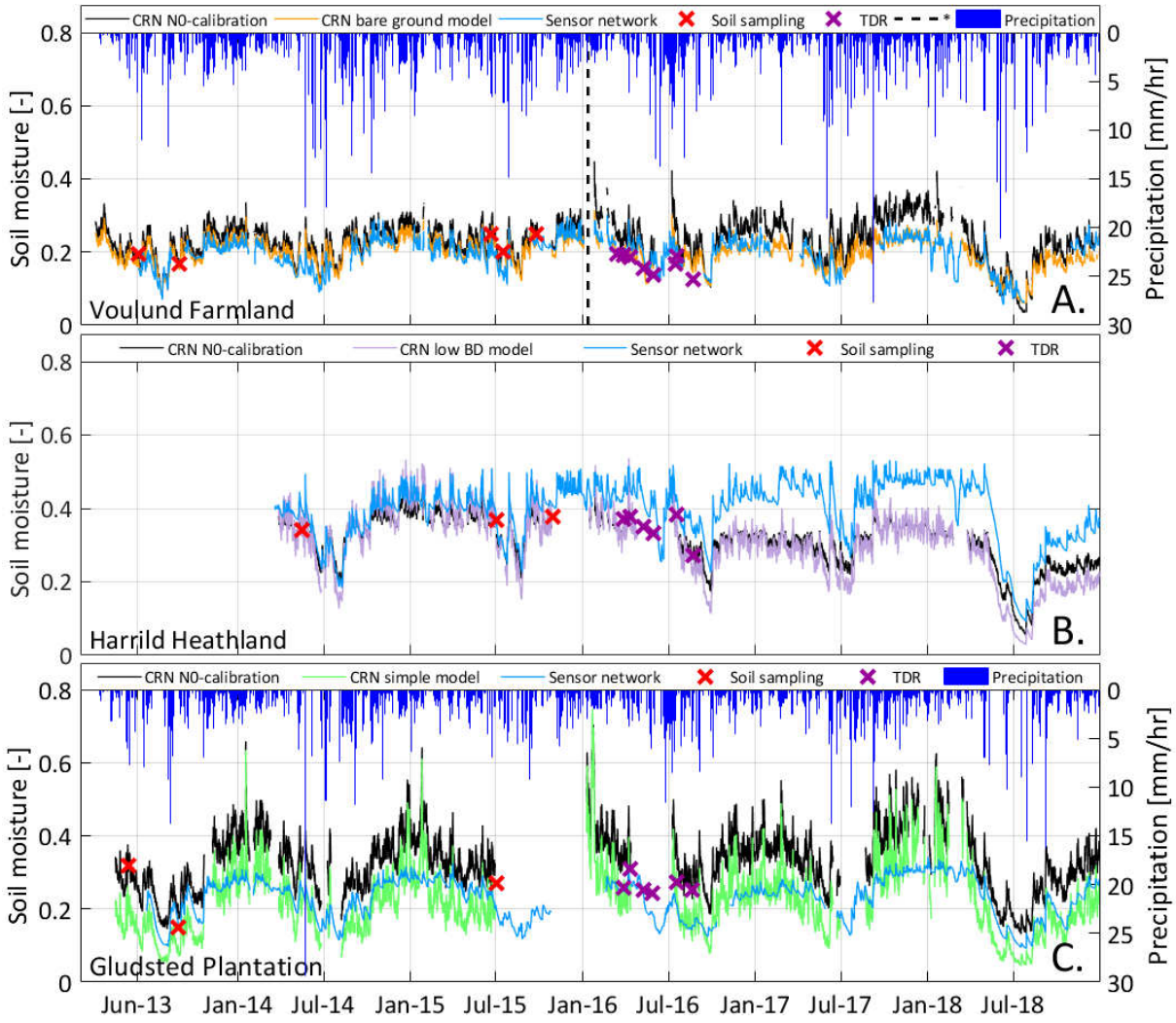
CRN N0-calibration
CRN bare ground model
Sensor network
Soil sampling
TDR
Precipitation
Soil moisture [-]
Precipitation [mm/hr]
Voulund Farmland
A.
CRN N0-calibration
CRN low BD model
Sensor network
Soil sampling
TDR
Harrild Heathland
B.
CRN N0-calibration
CRN simple model
Sensor network
Soil sampling
TDR
Precipitation
Gludsted Plantation
C.
Jun-13
Jan-14
Jul-14
Jan-15
Jul-15
Jan-16
Jul-16
Jan-17
Jul-17
Jan-18
Jul-18

Figure 6.


CRN N0-calibration
CRN bare ground model
Sensor network
Precipitation
Soil moisture [-]
Precipitation [mm/hr]
Voulund Farmland
A.
CRN N0-calibration
CRN low BD model
Sensor network
Harrild Heathland
B.
CRN N0-calibration
CRN simple model
Sensor network
Precipitation
Gludsted Plantation
C.
0
0.1
0.2
0.3
0
5
10
15
20
1/6-18
15/6-18
1/7-18
15/7-18
1/8-18
15/8-18
1/9-18